Russian Chemical Reviews **74** (3) 249 – 264 (2005) © 2005 Russian Academy of Sciences and Turpion Ltd

DOI 10.1070/RC2005v074n03ABEH000925

Structures and properties of spatially distorted porphyrins

O A Golubchikov, S G Pukhovskaya, E M Kuvshinova

Contents

I.	Introduction	249
II.	Structural characteristics	249
III.	Physicochemical properties	255
IV.	Coordination properties	261

Abstract. The published data on the structures and properties of porphyrins with distorted aromatic macrocycles are generalised and analysed. Data on the crystal structures, spectra and kinetics of formation and dissociation of their coordination derivatives are summarised. It is demonstrated that the distortion of the planar structure of the tetrapyrrole core is one of the most efficient means of controlling spectral, physicochemical and coordination properties of these compounds. The bibliography includes 95 references.

I. Introduction

That the tetrapyrrole rings of porphyrins (H_2P) are non-planar was demonstrated for the first time more than 30 years ago based on the data from X-ray diffraction analysis.[1–4] Generalisation of X-ray diffraction data has led Hoard [5] to conclude that the non-planarity of porphyrins and their metal derivatives (MP) is their common feature. Yet another important conclusion was that the size of the coordination centre of the porphyrin core is limited due to its cyclic structure. Radial distortion of the macrocycle is a minimum where the radius of the central cavity is ~200 pm. Any change in the size of the coordination cavity brings about distortion of the planar structure of the porphyrin macrocycle. These pioneering studies have formed the basis of conformational description of porphyrins.

In 1971, Hambright [6] proposed a mechanism of coordination of porphyrins by metal cations; its key idea was high deformability of the porphyrin macrocycle. Presumably, the Hambright mechanism is inapplicable for non-aqueous solutions;[7] however, distortion of the porphyrin core is obviously one of the most efficient mechanisms of controlling physicochemical, coordination and catalytic properties of porphyrins.

Distortion of porphyrin molecules (here, we imply distortion of the planar structures of their tetrapyrrole cores) can be achieved in various ways, *e.g.*, by introducing a large number of peripheral substituents or short spacers that form bridges between the *meso*- or β-positions or by protonation, *N*-alkylation or *N*-arylation of the coordination centre. Metalloporphyrins also contain distorted macrocycles; the role of complex-forming agents is played by bulky and some highly charged cations. The main emphasis in this review will be laid on the porphyrins distorted due to peripheral substitution.

In the 1990's, Smith *et al.*[8] synthesised and characterised a large series of porphyrins containing up to 12 peripheral substitutents as well as *N*-alkyl derivatives and porphyrins containing bulky *meso*-substituents inducing deformation of the tetrapyrrole core. The methods for the synthesis of this type of compounds have been reviewed.[9]

Analysis of NMR spectra revealed that in the majority of cases the structural parameters of such porphyrins are not changed on going from the crystalline state to solution, *i.e.*, distortion of polysubstituted porphyrins is a result of steric strains in the porphyrin molecules due to intramolecular interactions rather than intermolecular forces in crystals. If direct methods, *e.g.*, X-ray diffraction analysis or NMR, cannot be used, the structure of porphyrins can be deduced from calculations by molecular mechanics methods (MM), which reflect adequately their molecular geometry provided that competent approaches are used.

II. Structural characteristics

Conformational flexibility of porphyrins can be exemplified by structurally simple compounds, such as tetraphenylporphine (**1**), octaethylporphine (**2**) and their nickel complexes (NiP). These compounds were obtained in the crystalline state with both planar and non-planar structures of their cores.[1,2,10–14] The X-ray diffraction data summarised in Table 1 suggest that in the tetragonal modifications the mean deviation of the C and N atoms of the porphyrin skeleton from the mean-square plane passing through 24 atoms (Δ24) is ~20 pm. The *meso*-carbon atoms (C_{ms}) are at the largest distance from this plane (50 pm).[1,10]

Coordination of porphyrins by the d^8-nickel cation, which has a small radius in the low-spin state, leads to further distortion of the core and formation of a non-planar ruffled conformation where the pyrrole rings are tilted about the axes $C_\alpha - C_\alpha$ eventually resulting in a significant displacement of the C_{ms} atoms. Two crystalline forms, *viz.*, the planar triclinic [11] and the highly ruffled tetragonal [10] forms of NiP (**2**), were first detected. Yet another planar triclinic modification of NiP (**2**) was described later.[14] The deviations of the carbon and nitrogen atoms from the mean planes of the macrocycles of NiP (**1**) and NiP (**2**) are shown in Fig. 1.

O A Golubchikov, E M Kuvshinova Ivanovo State University of Chemistry and Technology, prosp. F Engelsa 7, 153460 Ivanovo, Russian Federation. Fax (7-0932) 41 79 95, tel. (7-0932) 32 73 78, e-mail: golubch@isuct.ru (O A Golubchikov), tel. (7-0932) 33 25 43 (E M Kuvshinova)
S G Pukhovskaya Institute of Solution Chemistry, Russian Academy of Sciences, ul. Akademicheskaya 1, 153045 Ivanovo, Russian Federation. Fax (7-0932) 33 62 37, tel. (7-0932) 33 69 90, e-mail: puhovskaya@isuct.ru (S G Pukhovskaya)

Received 30 March 2004
Uspekhi Khimii **74** (3) 268 – 284 (2005); translated by R L Birnova

Table 1. Structural characteristics of tetraphenylporphine (**1**), octaethylporphine (**2**) and their nickel complexes.

A. Bond lengths /pm

Porphyrin	M–N	N–C_α	C_α–C_β	C_α–C_{ms}	C_β–C_β	C_{ms}–C_{Ph}	Ref.
H_2P (**1**), tetragonal	–	135.0(7)	143.8(8)	140.3(7)	136.2(9)	151.4	1
H_2P (**1**), triclinic	–	137.2	144.2	140.0	135.1	150.3	2
H_2P (**2**)	–	136.6(2)	145.1(2)	139.2(2)	136.8(2)	–	12
NiP (**1**)	193.1(2)	137.7(3)	142.9(3)	138.2(4)	134.0(4)	149.9(3)	13
NiP (**2**), tetragonal	192.9(3)	138.6(2)	144.9(5)	137.2(2)	136.2(2)	–	10
NiP (**2**), triclinic	195.8(2)	137.6(4)	144.3(3)	137.1(4)	134.6(2)	–	11

B. Bond angles /deg

Porphyrin	N–M–N	M–N–C_α	N–C_α–C_{ms}	N–C_α–C_β	C_α–N–C_α	C_α–C_{ms}–C_α	C_α–C_β–C_β	C_{ms}–C_α–C_β	Ref.
H_2P (**1**), tetragonal	–	–	126.0(5)	107.5(4)	108.9(4)	125.2(5)	106.9(5)	125.1(5)	1
H_2P (**1**), triclinic	–	–	126.2	108.8	107.7	125.6	107.5	124.9	2
H_2P (**2**)	–	–	125.1(1)	109.4(1)	107.7(1)	127.6(1)	106.8(1)	125.7(1)	12
NiP (**1**)	90.0	127.5(2)	125.5(2)	110.4(2)	104.9(2)	120.0(2)	107.1(2)	123.9(2)	13
NiP (**2**), tetragonal	90.0	127.4(2)	124.0(2)	110.6(2)	105.1(3)	124.1(2)	106.8(3)	125.0(2)	10
NiP (**2**), triclinic	90.2(1)	128.0(2)	124.4(3)	111.6(3)	103.9(2)	125.1(3)	106.5(3)	124.1(3)	11

C. Inclination of the pyrrole and phenyl fragments relative to, and deviation of the atoms from, the mean plane of the macrocycle.

Porphyrin	Inclination /deg		Deviation of the atoms from the mean plane of the macrocycle /pm						Ref.
	φ_{pyr}	φ_{Ar}	*R* (see [a])	Δ24	ΔN	ΔC_{ms}	ΔC_α	ΔC_β	
H_2P (**1**), tetragonal	11.5	78.5	205.4	19	4	38	21	14	1
H_2P (**1**), triclinic	7.5	60.0	206	5	0	4	2	3	2
H_2P (**2**)	1.7	–	206.2	2	0	4	2	8	12
NiP (**1**)	14.4	78.7	193.1	22	1	45	26	18	13
NiP (**2**), tetragonal	16.4	–	192.9	26	1	51	30	27	10
NiP (**2**), triclinic	1.7	–	195.8	2	0	3	7	6	11

[a] Hereinafter, *R* is the radius of the coordination plane of the porphyrin core.

Octasubstituted tetraphenylporphines containing alkyl, cycloalkyl groups and halogens in the β-positions are studied in most detail in comparison with other porphyrins distorted due to the presence of a large number of peripheral substituents. The structural characteristics of β-octaethyl-*meso*-tetraphenylporphine (**3**) and its complexes obtained by X-ray diffraction analysis and MM are listed in Table 2.[15–19]

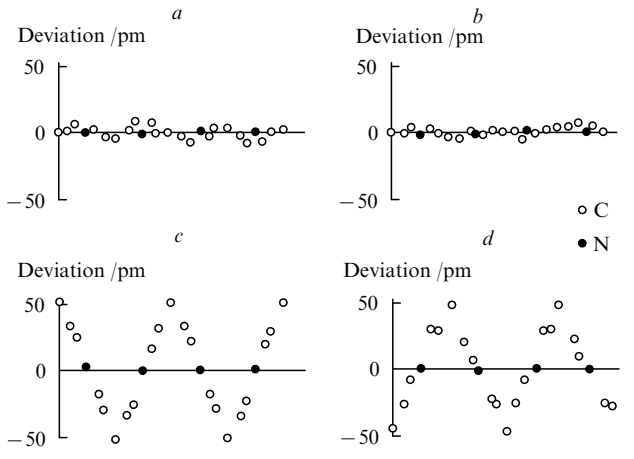


Figure 1. Deviations of carbon and nitrogen atoms from the mean plane passing through 24 atoms of the tetrapyrrole macrocycle in nickel complexes of octaethylporphine and tetraphenylporphine.
(*a*) NiP (**2**) triclinic,[11] (*b*) NiP (**2**) triclinic,[14] (*c*) NiP (**2**) tetragonal,[10] (*d*) NiP (**1**).[13]

The macrocyclic core of β-octaethyl-*meso*-tetraphenylporphine and its coordination compound has a symmetric saddle shape. A characteristic feature of this conformation is that two opposite pyrrole cores are raised above the mean plane of the molecule, while the other two are depressed as a result of the van der Waals repulsions of the *meso*-phenyl and alkyl groups; such *meso*-carbon atoms are coplanar with the macrocycle. This type of deformation is also characteristic of octamethyl analogues, *e.g.*, CuP (**3**) (see Ref. 16) and zinc β-octamethyl-*meso*-tetraphenylporphine pyridinate Zn(Py)P (**4**) † (see Ref. 19). Both complexes possess substantially distorted macrocycles, the differences between the methyl and ethyl derivatives being insignificant (Fig. 2).

The deviation of C_β-atoms owing to sequential up-and-down displacement of the pyrrole rings relative to the mean-square plane (the torsion angle is ~30°) reaches 109–115 pm. Compared to tetraphenylporphin, the *meso*-phenyl rings of its β-octaalkyl-substituted derivatives are rotated by a smaller angle relative to the mean plane of the macrocycle (43–46°); however, this does not result in any significant decrease in the lengths of the C_{ms}–C_{Ph} bonds. Such a structural type is characteristic of all tetraphenylporphine derivatives containing methyl, ethyl, propyl and cycloalkyl substituents in the β-positions. It is noteworthy

† Coordinated acido- and molecular ligands are indicated in parentheses after the metal cation; crystallisation molecules of the solvent stand after a dot. For example: Zn(Py)P (**1**) · 2 MeOH.

Table 2. Structural characteristics of β-octaethyl-*meso*-tetraphenylporphine (**3**) and its metallocomplexes.

A. Bond lengths /pm

Porphyrin	$M-L_{ax}$	M–N	$N-C_\alpha$	$C_\alpha-C_\beta$	$C_\alpha-C_{ms}$	$C_\beta-C_\beta$	$C_{ms}-C_{Ph}$	Ref.
H_2P (**3**)	–	–	136.8	145.1	140.7	137.7	–	15
Fe(Cl)P (**3**)	224.2(2)	203.1(5)	138.6(7)	144.9(9)	140.5(8)	136.0(9)	152.4(8)	16
CoP (**3**)	–	192.9(3)	138.2(6)	145.7(7)	140.2(7)	136.2(7)	–	16
NiP (**3**)	–	190.6(2)	138.1(2)	145.1(3)	139.5(2)	136.5(5)	149.1(1)	17
CuP (**3**)	–	197.3(4)	137.9(6)	145.5(7)	140.3(7)	136.7(7)	149.3(7)	18
CuP (**3**) · 2 CH_2Cl_2	–	197.7(5)	137.8(8)	145.8(8)	140.4(8)	136.8(8)	–	16
CuP (**3**) (see [a])	–	197.4(3)	138.3(6)	144.4(6)	140.7(6)	136.7(7)	149.0(7)	18
Zn(MeOH)P (**3**)	222.6(5)	206.3(5)	137.1(2)	146.1(2)	141.6(3)	137.0(7)	–	19

B. Bond angles /deg

Porphyrin	N–M–N	$M-N-C_\alpha$	$N-C_\alpha-C_{ms}$	$N-C_\alpha-C_\beta$	$C_\alpha-N-C_\alpha$	$C_\alpha-C_{ms}-C_\alpha$	$C_\alpha-C_\beta-C_\beta$	$C_{ms}-C_\alpha-C_\beta$	Ref.
H_2P (**3**)	–	–	122.4	108.7	108.6	123.8	106.9	128.8	15
Fe(Cl)P (**3**)	87.1(2)	122.8(4)	121.5(5)	109.4(5)	106.2(1)	123.0(5)	107.2(5)	128.8(5)	16
CoP (**3**)	90.5(2)	125.6(3)	121.7(4)	110.0(4)	105.6(4)	122.2(5)	106.7(4)	127.9(5)	16
NiP (**3**)	90.6(2)	125.3(2)	121.3(2)	109.8(1)	105.9(2)	121.4(1)	106.8(1)	128.3(1)	17
CuP (**3**)	90.3(2)	124.5(3)	121.8(4)	109.5(4)	106.7(4)	123.2(4)	106.8(4)	128.4(5)	18
CuP (**3**) · 2 CH_2Cl_2	90.3(2)	124.7(4)	122.0(4)	109.6(4)	106.6(5)	123.4(5)	107.0(5)	128.1(5)	16
CuP (**3**) (see [a])	89.9(2)	121.2(4)	119.8(4)	110.5(4)	105.3(4)	121.1(3)	106.7(4)	129.5(4)	18
Zn(MeOH)P (**3**)	89.4(4)	122.9(6)	122.4(2)	109.2(3)	107.7(4)	124.4(4)	106.8(2)	128.2(2)	19

C. Inclination of the pyrrole and phenyl fragments relative to, and deviation of the atoms from, the mean plane of the macrocycle.

Porphyrin	Inclination /deg		Deviation of the atoms from the mean plane of the macrocycle /pm							Ref.
	φ_{pyr}	φ_{Ar}	*R*	Δ24	ΔM	ΔN	ΔC_{ms}	ΔC_α	ΔC_β	
H_2P (**3**)	31.2	43.2	205.1	54	–	7	3	42	117	15
Fe(Cl)P (**3**)	29.8	44.9	197.6	58	47	11	19	44	115	16
CoP (**3**)	27.5	46.1	192.0	58	1	18	5	47	117	16
NiP (**3**)	29.4	43.4	190.6	62	1	19	3	52	124	17
CuP (**3**)	28.2	45.6	197.3	57	0	14	5	45	115	18
CuP (**3**) · 2 CH_2Cl_2	27.4	46.9	197.3	55	0	14	4	44	112	16
CuP (**3**) (see [a])	37.3	33.1	197.2	66	9	4	20	49	135	18
Zn(MeOH)P (**3**)	28.4	46.1	206.3	51	22	6	4	39	109	19

[a] The radical cation form of the copper complex with perchlorate as a counterion.

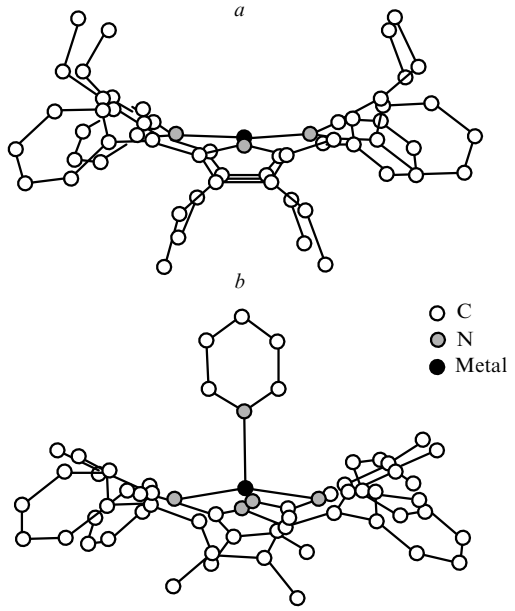


Figure 2. Structures of the copper complex of β-octaethyl-*meso*-tetraphenylporphine (*a*)[16] and zinc β-octamethyl-*meso*-tetraphenylporphine pyridinate (*b*).[19]

that the saddle conformation of the β-octamethyl-*meso*-tetraphenylporphine (**4**) macrocycle is slightly ruffled (Fig. 3).

The shapes of the tetrapyrrole macrocycles of distorted porphyrins are rather diverse (Fig. 4).[20] In addition to the aforementioned saddle and ruffled structures, two wavelike, dome-shaped and propeller conformations are also known. In the majority of cases, the shape of the tetrapyrrole core of a distorted porphyrin can be described by one of the above-mentioned types or their combination.

Dodecasubstituted porphyrins and their planar analogues differ in the angles between the same type of bonds (see Tables 1 and 2). The increase in the $C_{ms}-C_\alpha-C_\beta$ angles and the decrease in the $N-C_\alpha-C_{ms}$ and $M-N-C_\alpha$ angles in the distorted porphyrins by 3–4° in comparison with planar porphyrins are the most significant. This peculiarity is characteristic of all metalloporphyrins **3** (see Tables 1 and 2). Using nickel complexes of highly substituted porphyrins as an example, it was shown[4] that these parameters correlate with the degree of the non-planarity of the macrocycle.

Studies of the structure of Zn(Py)P (**4**) revealed[19] that the conformation of the macrocycle depends on the axial ligands. The displacement of the C_β atoms of the pyrrole rings close to the axial ligand is less pronounced (90 pm) than that of the opposite C_β atoms of the pyrrole cores (120 pm).

In the case of dodecasubstituted porphyrin complexes with 3d-metals, the degree of non-planarity of the tetrapyrrole macro-

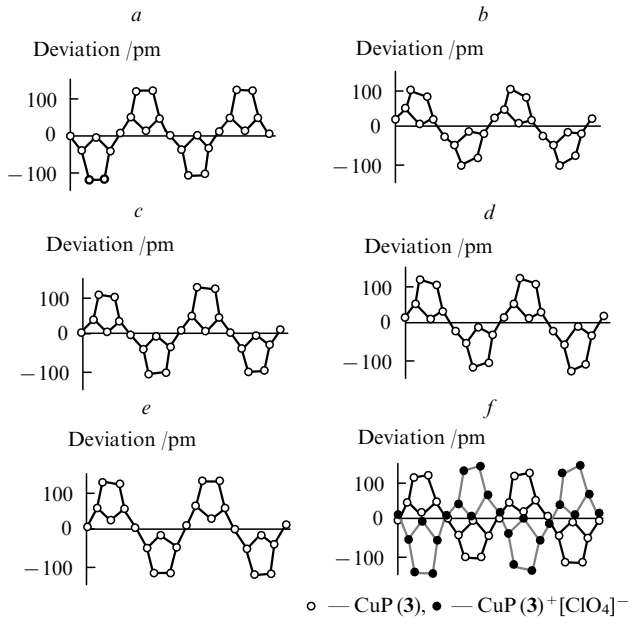


Figure 3. Deviations of carbon and nitrogen atoms in dodecasubstituted porphyrins and metalloporphyrins from the mean plane of the macrocycle.
(*a*) H_2P (**3**), (*b*) H_2P (**4**), (*c*) ZnP (**4**)·MeOH, (*d*) Fe(Cl)P (**3**), (*e*) NiP (**3**), (*f*) CuP (**3**) and its radical-cation form.[15]

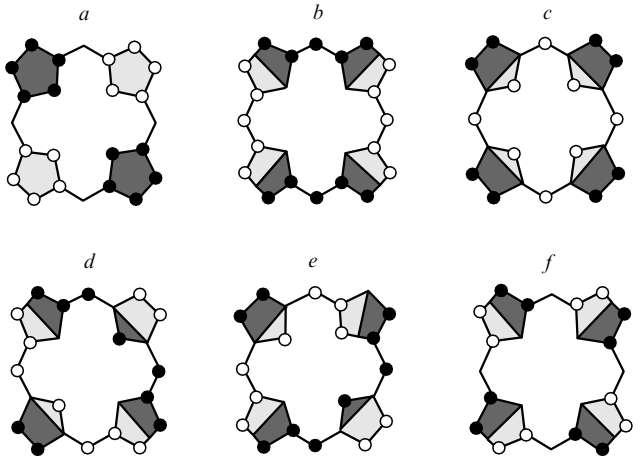


Figure 4. Typical conformations of non-planar porphyrins.
(*a*) saddle-shaped, (*b*) ruffled, (*c*) dome-shaped, (*d*, *e*) wave-shaped, (*f*) propeller-shaped. The unshaded fragments lie above the mean plane of the macrocycle, the dark fragments lie under it.[20]

cycle depends on the size of the complex-forming atom (see Table 2). Judging from the displacement of N, C_α and C_β atoms relative to the mean plane of the macrocycle, the distortion of the macrocycle decreases with an increase in the size of the metal cation in the series from Ni^{2+} (69 pm) to Zn^{2+} (74 pm). In this case, the lengths of the M—N and C_α—C_{ms} bonds increase, while those of the N—C_α bonds decrease; the angles between the M—N—C_α bonds decrease, while those between the C_α—N—C_α and C_α—C_{ms}—C_α bonds increase. The changes in other structural parameters of metalloporphyrins on going from the smallest to the largest metal atom are insignificant and do not exceed 1 pm or 1°. It is of note that complexes of spatially distorted porphyrins with cations the sizes of which differ substantially from those of 3d-metals have not been investigated yet.

Similarly, the geometry of the complexes of the non-strained planar porphyrins **1** and **2** with 3d-metal cations depends on the sizes of these cations. The sizes of the coordination cavities of porphyrins decrease with an increase in the degree of distortion of the tetrapyrrole core. In turn, coordination of porphyrins by small cations results in further distortion of the macrocycle (Fig. 5).[16] It should be kept in mind, however, that coordination of porphyrins by cations having very large sizes, *e.g.,* Pt(II),[21] In(III)[22] or Tl(III),[23] also results in the distortion of the tetrapyrrole cores of metalloporphyrins. According to spectral measurements and calculations, distortions of polysubstituted porphyrins are retained on going from the crystalline state to solution.[24–32]

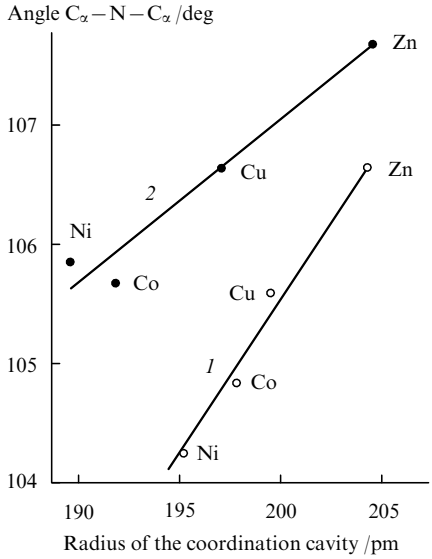


Figure 5. Relationship between the radius of the coordination cavity and the bond angle C_α—N—C_α of octaethylporphine (*1*) and β-octaethyl-*meso*-tetraphenylporphine (*2*) complexes.[16]

Porphyrins halogenated in the β-positions constitute a large group of spatially distorted dodecasubstituted compounds. The tetrapyrrole cores in copper[33] and nickel[33,34] complexes of β-octabromo-*meso*-tetrakis(pentafluorophenyl)porphine (**5**) and β-octabromo-*meso*-tetramesitylporphine (**6**) and its nickel complex have a saddle conformation. The average distances of the C_{ms}, C_β and Br atoms from the plane formed by four nitrogen atoms for the copper and nickel complexes of porphyrin **5** are 16.3, 112 and 199 pm and 18.7, 118 and 205 pm, respectively.[33] Very short contacts Br—Br and Br—$C(1)_{Ph}$ were observed; the sums of the van der Waals radii of these pairs of atoms exceed the real distances between them by ~45 pm. However, the lengths of the C—N and C—C bonds in the β-halogenated complexes are virtually the same as those of metalloporphyrins devoid of steric strains. Some structural characteristics of copper and nickel complexes of the porphyrin **5** are listed in Table 3. In these complexes, one of the two bromine atoms in each pair occupying the β-position of the pyrrole ring is more remote from the mean plane of the macrocycle than the other atom. Bulky *ortho*-substituents in the benzene rings of porphyrins **5** and **6** and the neighbouring halogen β-atoms form cavities on both sides of the porphyrin core (Fig. 6).[34] This restricts spatial arrangements of the ligands additionally coordinated by metalloporphyrins[26,28,29,35] and can be directly related to high and specific catalytic activity of polyhalogenated porphyrin complexes with iron(III) in oxidation processes.[36–43]

Dodecaarylporphine derivatives pertain to the class of porphyrins with the most strongly distorted macrocycle. Dodecaphenylporphine (**7**) has a saddle conformation with two highly asymmetric pairs of pyrrole rings in crystals with rhombohedral

Table 3. Bond lengths and bond angles in copper and nickel complexes of β-octabromo-*meso*-tetrakis(pentafluorophenyl)porphine.[33]

Bond	Bond length /pm		Bond angle	Angle magnitude /deg	
	for NiP (**5**)	for CuP (**5**)		for NiP (**5**)	for CuP (**5**)
$M-N_1$	190.2(4)	196.9(6)	N_2-M-N_1	90.5(2)	90.1
$M-N_2$	190.4(4)	197.7(6)	N_3-M-N_1	168.4(2)	171.0
$M-N_3$	189.8(4)	197.1(6)	N_4-M-N_1	90.8(2)	91.2
$M-N_4$	190.6(4)	196.8(6)	N_3-M-N_2	90.3(2)	89.9
$Br-C_2$	185.8(6)	188.4(7)	N_4-M-N_2	168.5(2)	171.5
$Br-C_3$	187.2(6)	188.7(8)	N_4-M-N_3	90.8(2)	90.2
$Br-C_7$	186.3(6)	187.4(8)			
$Br-C_8$	187.1(6)	186.7(8)			
$Br-C_{12}$	188.0(6)	185.6(8)			
$Br-C_{13}$	186.1(6)	188.2(8)			
$Br-C_{17}$	187.0(6)	188.5(8)			
$Br-C_{18}$	187.1(6)	187.0(8)			

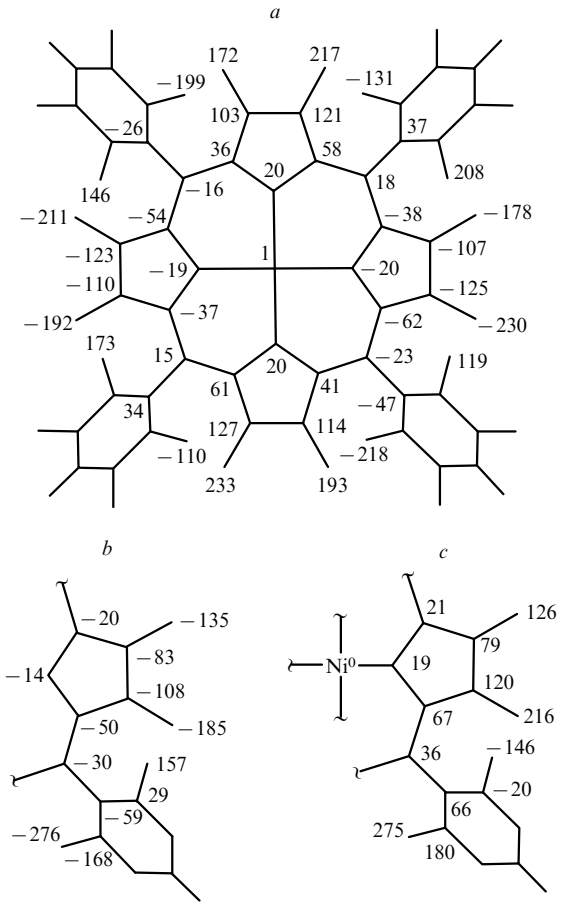


Figure 6. Deviations of atoms (pm) from the mean plane of the tetrapyrrole macrocycle in a nickel complex of β-octabromo-*meso*-tetrakis(pentafluorophenyl)porphine (*a*), β-octabromo-*meso*-tetramesitylporphine (*b*) and its nickel complex (*c*).[34]

modification (Figs. 7 and 8 *a*).[44] Analysis of intra- and intermolecular interactions revealed[44] that the distortion of the macrocycle in this modification is due to the intramolecular repulsion of the phenyl substituents rather than to the crystal packing effects. Later, two new crystalline forms of dodecaphenylporphine, *viz*., the triclinic form[45] [H_2P (**7**)$\cdot 2\,EtOH\cdot 2\,CH_2Cl_2$] with a configuration similar to that described above (Fig. 8 *b*) and a much more symmetric rhombohedral conformation [H_2P (**7**)$\cdot 3\,H_2O$], were found.[46] The latter has a saddle shape; its C_β atoms are displaced

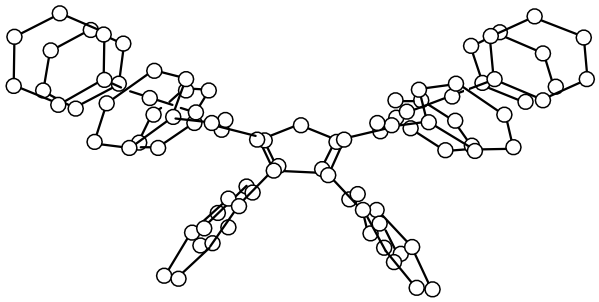


Figure 7. Structure of dodecaphenylporphine of rhombohedral crystals of H_2P (**7**)$\cdot 3\,CH_2Cl_2$ (the hydrogen atoms are not shown).[44]

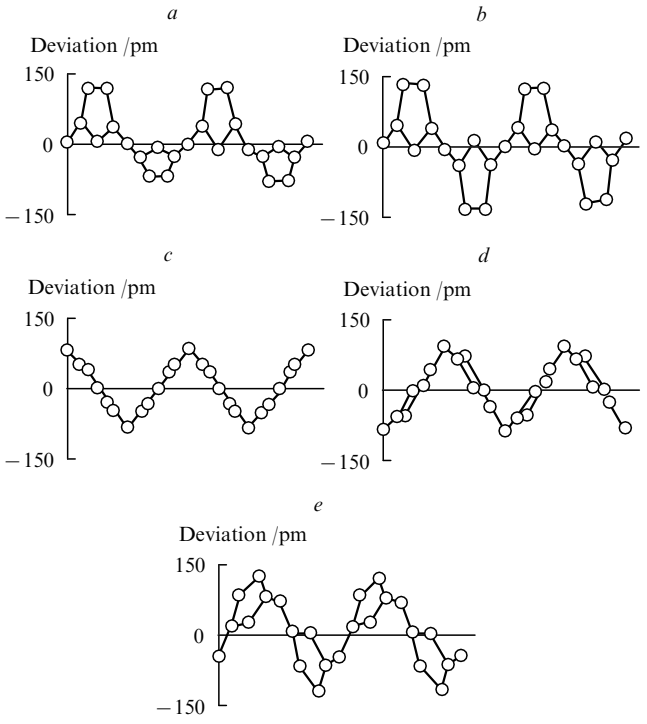


Figure 8. Deviations of carbon and nitrogen atoms in different crystalline modifications of dodecaphenylporphine and its nickel complex from the mean plane passing through 24 atoms of the tetrapyrrole macrocycle.[44–46]
(*a*) H_2P (**7**)$\cdot 3\,CH_2Cl_2$ rhombohedral, (*b*) H_2P (**7**)$\cdot 2\,CH_2Cl_2\cdot 2\,EtOH$ triclinic, (*c*) NiP (**7**)$\cdot 5.8\,C_6H_{12}\cdot 0.9\,CHCl_3$ cubic, (*d*) NiP (**7**)$\cdot 3.5\,CHCl_3$ rhombohedral and NiP (**7**)$\cdot 1.5\,H_2O$, (*e*) NiP (**7**) rhombohedral.

by 132 pm relative to the mean plane of the tetrapyrrole core,[46] which markedly exceeds the corresponding parameter for β-octaethyl-*meso*-tetraphenylporphine H_2P (**3**) (117 pm).[15] Some structural characteristics of the porphyrin **7** and its complexes are listed in Table 4; it can be seen that the macrocycle of the dodecaphenyl-substituted porphyrin is more flexible than that of octaalkyltetraphenyl derivatives. For example, four crystalline forms of NiP (**7**) differing notably from one another have been established. The cubic form has a purely ruffled configuration; its C_{ms} atoms are displaced relative to the mean plane of the macrocycle by 86 pm (Fig. 8 *c*).[45] The rhombohedral modification of a solvate containing 3.5 molecules of $CHCl_3$, albeit also ruffled, has an entirely different shape (Fig. 8 *d*). In this case, two C_β atoms in each pyrrole ring are displaced asymmetrically by 70 and 10 pm, while the deviation of the *meso*-atoms projecting from the mean plane of the macrocycle is as large as before.[46] Yet another crystal solvate, *viz*., NiP (**7**)$\cdot 1.5\,H_2O$, described in[46] has a similar conformation. And, finally, the fourth crystal modification,

Table 4. Structural characteristics of dodecaphenylporphine and its complexes.[44–46]

Porphyrin	Bond length M–N /pm	φ_{pyr} /deg	$\varphi_{ms(Ar)}$ /deg	Δ24 /pm	ΔM /pm	ΔN /pm	ΔC_{ms} /pm	ΔC_{β} /pm
H_2P (**7**) · 3 CH_2Cl_2	–	18.0; 33.6	43.8	–	–	14; 1	0	78; 120
H_2P (**7**) · 3 H_2O	–	–	–	60	–	7	5	132
H_2P (**7**) · 2 EtOH · 2 CH_2Cl_2	–	40.9	22.0	60	–	10	7	132
NiP (**7**) · 5.8 C_6H_{12} · 0.9 $CHCl_3$	190.9	22.8	89.1	43	0	1	86	36
Ni (**7**)	188.5	–	–	60	6	13	60	76; 133
NiP (**7**) · 3.5 $CHCl_3$ and NiP (**7**) · 1.5 H_2O	189.4	–	–	45	2	4	92	70; 10
ZnP (**7**)	203.7	–	48	46	7	10	1	96

which corresponds to the non-solvated form of the tetrapyrrole macrocycle represents a combination of ruffled and saddle conformations with a shift of the *meso*-carbon atoms from the mean plane by 60 pm and a non-symmetric shift of the C_{β} atoms by 76 and 133 pm (Fig. 8 *e*).[46]

Tetraphenylporphine derivatives containing from two to six ethyl groups in the β-positions were synthesised and characterised by X-ray diffraction.[47] The structural characteristics of 2,3-diethyl- (**8**), 2,3,7,8-tetraethyl- (**9**), 2,3,12,13-tetraethyl- (**10**) and 2,3,7,8,12,13-hexaethyl-5,10,15,20-tetraphenylporphine (**11**) and their nickel(II), copper(II) and zinc(II) complexes are listed in Table 5. For the sake of comparison, the corresponding parameters for tetraphenylporphine (**1**) and octaethyltetraphenylporphine (**3**) are also given. As expected, the degree of distortion of the tetrapyrrole macrocycle increases with an increase in the number of peripheral substituents. Of two tetraethyltetraphenylporphine derivatives, the non-symmetrical isomer **9** is distorted to a much greater degree than the symmetrical isomer **10**. All porphyrins of this series have a saddle conformation of the macrocyclic core (Fig. 9).

The planar structure of the macrocycle extended along the axis C(5)–C(15) is retained in the molecules of symmetrical 2,3,5,7,8,12,13,15,17,18-decaalkylporphines and 5,15-diaryl-β-octaalkylporphines.[48,49] At the same time, copper and nickel complexes of these porphyrins are subject to extraplanar distortion: their tetrapyrrole macrocycles are folded along the axis C(5)–C(15) and have a gable roof conformation.[49–52] Non-symmetrical 5,10-di- and 5,10,15-trisubstituted porphyrins are highly distorted.[49] The conformations of their macrocycles represent a combination of ruffled and saddle-like distortions.

Macrocycles of porphyrins containing only four substituents can also be distorted. Zinc *meso*-tetra-*tert*-butylporphine pyridinate (**12**) has a strongly ruffled aromatic core (Fig. 10).[53,54] Nickel

Table 5. Structural characteristics of tetraphenylporphine and its β-ethyl derivatives.

Compound	Δ24 /pm	ΔC_{β} /pm	ΔC_{ms} /pm	φ_{pyr} /deg	*R* /pm	ΔM /pm	Ref.
H_2P (**1**) triclinic	5	6	4	4.0	206	–	2
H_2P (**1**) tetragonal	19	14	38	11.9	205.4	–	1
H_2P (**8**)	10	19	5	4.3	206.4	–	47
H_2P (**10**)	29	61	4	15.0	205.7	–	47
H_2P (**9**)	38	76	12	20.4	207.0	–	47
H_2P (**11**)	46	95	6	24.0	204.9	–	47
H_2P (**3**)	54	117	3	31.2	205.1	–	15
NiP (**8**)	45	82	28	21.0	192.3(6)	0	47
NiP (**10**)	39	32	79	25.7	189.3(6)	3	47
	46	61	68	26.1	189.3(6)	0	47
NiP (**9**)	49	89	20	20.8	192.3(4)	1	47
Ni (**11**)	53	100	16	23.4	192.1(3)	1	47
Ni (**3**)	62	125	3	29.4	190.6(2)	1	17
Cu (**1**)	21	16	42	13.4	198.1(7)	0	5
CuP (**8**)	32	58	16	13.9	199.0(3)	5	47
	26	52	7	12.2	199.9(3)	2	47
CuP (**10**)	40	73	23	18.1	198.4(4)	2	47
CuP (**9**)	44	83	17	19.8	197.5(5)	2	47
CuP (**11**)	49	95	13	23.0	198.0(5)	2	47
CuP (**3**)	55	113	4	27.4	197.7(5)	0	18
ZnP (**1**) · H_2O	1	0	0	0	205.0(3)	17	5
ZnP (**1**) triclinic	5	21	15	6.5	203.7(3)	0	5
ZnP (**8**) · MeOH	6	12	2	3.1	206.2(5)	21	47
ZnP (**8**) · (β-pic) [a]	18	25	17	9.3	206.8(4)	32	47
ZnP (**10**) · Py	28	54	20	15.0	207.1(3)	31	47
ZnP (**9**) · Py	33	63	18	16.9	207.0(3)	32	47
ZnP (**11**)	45	84	12	22.5	202.8(4)	7	47
ZnP (**11**) · Py	43	89	6	22.4	206.9(3)	35	47
ZnP (**3**) · MeOH	50	109	4	28.4	206.3(5)	22	19

[a] β-pic is β-picoline.

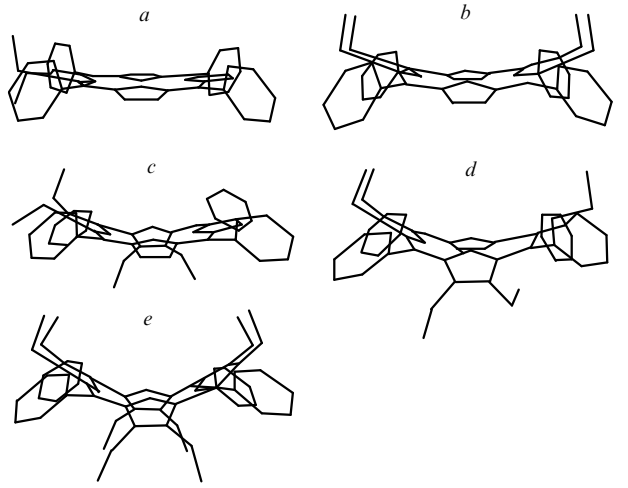


Figure 9. Structures of ethyltetraphenylporphine derivatives: (*a*) H_2P (**8**), (*b*) H_2P (**10**), (*c*) H_2P (**9**), (*d*) H_2P (**11**), (*e*) H_2P (**3**).[47]

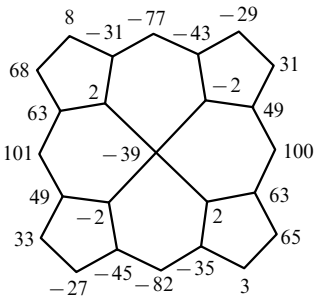


Figure 10. Deviation of the atoms (pm) from the mean plane of the macrocycle of Zn(Py)P (**12**).[53,54]

meso-tetraisopropylporphine manifests saddle-like distortion of the macrocycle.[53]

It is noteworthy that introduction of substituents into *meso*-positions brings about stronger deformation of the tetrapyrrole core of porphyrins in comparison with β-substitution.

III. Physicochemical properties

Distortion of the planar structure of the tetrapyrrole core strongly affects the spectral characteristics of porphyrins. The ^{1}H NMR spectra of octamethylporphine (**13**) and its *meso*-phenyl derivatives, *viz*., 5-phenyl- (**14**), 5,15-diphenyl- (**15**), 5,10-diphenyl- (**16**), 5,10,15-triphenyl- (**17**) and 5,10,15,20-tetraphenyl-2,3,7,8,12,13,17,18-octamethylporphine (**4**), have been analysed.[55] Symmetrical compounds of this series have extremely low solubility in neutral and basic solvents; therefore, their ^{1}H NMR spectra were recorded for solutions in deuteriochloroform with 0.5% trifluoroacetic acid. In this medium, porphyrins are easily soluble and exist in the protonated form.

As expected, the ^{1}H NMR spectrum of porphyrin **13** contained only three singlet peaks corresponding to the protons in the *meso*-positions, of the methyl and NH groups (Table 6). The ^{1}H NMR spectrum becomes more complicated on going to the monophenyl derivative **14** as can be evidenced from the splitting of the signals corresponding to the β-methyl groups and the appearance of peaks at $\delta \sim 8$ corresponding to protons of the phenyl substituents. The results of MM calculations of the porphyrin **14** structure (Fig. 11) suggest that the methyl groups in positions 3 and 7 lie in the region of the anisotropic shielding by the ring current of the phenyl nucleus. The signals for the protons of these methyl groups at $\delta \sim 2.3$ resonate and thus are upfield shifted by ~ 1.4 ppm in comparison with the corresponding signals in the ^{1}H NMR spectrum of octamethylporphine (**13**). The upfield shift of the signals by ~ 0.5 ppm was also observed for the neighbouring 2,8-groups and even for the 12,18-methyl groups. Obviously, these shifts cannot be only due to the anisotropic effect of the ring current of the phenyl residue. More probably, in this case two effects operate, *viz*., the negative inductive effect of the phenyl group and the effect of deformation of the porphyrin macrocycle. Introduction of the phenyl group decreases the strength of the ring current owing to the porphyrin macrocycle as can be judged from the upfield shift of the signals for the *meso*-protons and the downfield shift of the central NH group protons. Both signals are split into two components, the splitting being large for the NH groups (by 1.2 ppm) and small for the *meso*-protons (by 0.13 ppm). Judging from the integral intensity, the signal at δ 10.37 corresponds to the hydrogen atom in position 15, whereas the signal at δ 10.50 corresponds to the protons at the C(10) and C(20) atoms. This suggests that the splitting is due to the negative inductive effect of the phenyl substituent.

MM calculations of two diphenyloctamethylporphine derivatives have shown that the tetrapyrrole core of the symmetrical isomer **15** is distorted to a much lesser degree than that of its 5,10-substituted analogue **16** (Fig. 12). The ^{1}H NMR spectrum of porphyrin **15** (Table 6, Fig. 13 *a*) contains one singlet for the protons of the NH groups (δ −3.07), two singlets for the methyl groups (δ 2.27 and 3.26), a multiplet for the *meta*- and *para*-protons of the phenyl substituents (δ 7.94 – 7.97), a doublet for the *ortho*-protons (δ 8.23) and a singlet for the *meso*-protons (δ 10.34). A comparison of average values of the chemical shifts of the *meso*-protons of monophenyl- (**14**) and 5,15-diphenyloctamethylporphine derivatives (**15**) revealed that the strength of the ring current induced by the aromatic macrocycle of diphenylporphyrin is reduced. A similar conclusion can be derived from a comparison of positions of the protons of the NH groups in the ^{1}H NMR spectra of these porphyrins. Thus, introduction of the second phenyl substituent confers additional strain on the structure of the porphyrin macrocycle.

The ^{1}H NMR spectrum of the non-symmetrical porphyrin **16** is even more complicated (see Table 6 and Fig. 13 *b*). The protons of the central NH groups appear as three peaks at δ −3.84 (24-H), −2.23 (21, 23-H) and −1.31 (22-H); their assignment was based on the measurements of their integral intensities. The assignment of the protons of the methyl groups, which give four signals with the same integral intensities, was carried out taking account of the deshielding effect of the phenyl substituents on the neighbouring methyl groups: δ 1.81 — 7, 8-Me, δ 2.22 — 3, 12-Me, δ 3.23 — 2, 13-Me and δ 3.51 — 17, 18-Me. The *meso*-protons of the non-symmetrical porphyrin **16** resonate as a singlet at δ 9.99 and are shifted upfield in comparison with the symmetrical isomer **15**. At the same time, the protons of the NH groups of the porphyrin **16** are shifted downfield in comparison with compound **15**. The ^{1}H NMR spectrum of the neutral form of compound **16** recorded

Table 6. ^{1}H NMR spectra of octamethylporphine and its *meso*-phenyl derivatives in $CDCl_3$ with 0.5% CF_3CO_2H.[55]

Porphyrin	δ			
	meso-H	Me	Ph	NH
13	10.45, s	3.70, s	–	−4.45, s
14	10.50, s; 10.37, s	3.70, s (13, 17-Me); 3.26, s (2,8,12,18-Me); 2.27, s (3,7-Me)	8.22, m (*o*-H); 7.96, m (*m, p*-H)	−2.99, s; −4.21, s
15	10.34, s	3.26, s (2,8,12,18-Me); 2.27, s (3,7,13,17-Me)	8.22, d (*o*-H); 7.95, m (*m, p*-H)	−3.07, s
16	9.99, s	3.51, s (17,18-Me); 3.23, s (2,13-Me); 2.22, s (3,12-Me); 1.81, s (7,8-Me)	8.32, m (*o*-H); 7.95, m (*m, p*-H)	−1.31, s; −2.23, s; −3.84, s
17	9.79, s	3.13, s (2,18-Me); 2.24, s (3,17-Me); 1.84, s (7,8,12,13-Me)	7.98, m (*o*-H); 7.94, m (*m, p*-H)	−1.26, s; −2.47, s
4	–	1.84, s	8.35, m (*o*-H); 7.93, m (*m, p*-H)	−1.14, s

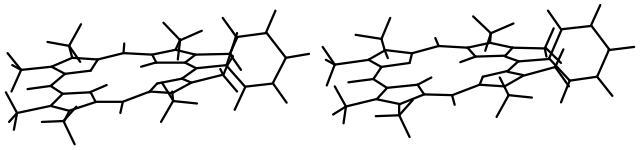


Figure 11. A stereo image of the structure of 5-phenyloctamethylporphine (**14**) optimised by the molecular mechanics method (force field MM +).[55]

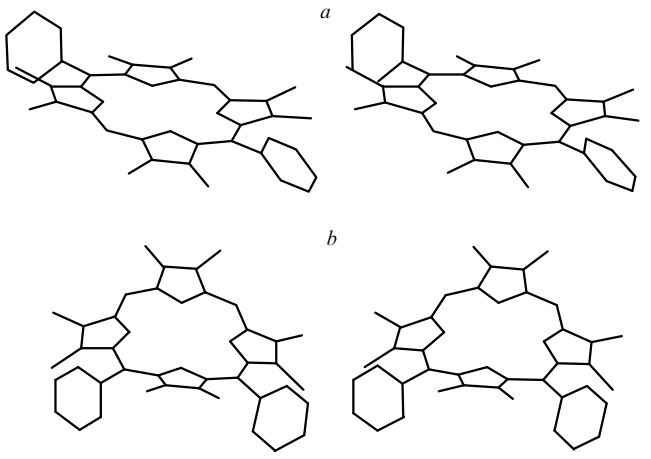


Figure 12. Stereo images of the structures of diphenyl derivatives of octamethylporphines **15** (*a*) and **16** (*b*) optimised by the molecular mechanics method.[55]

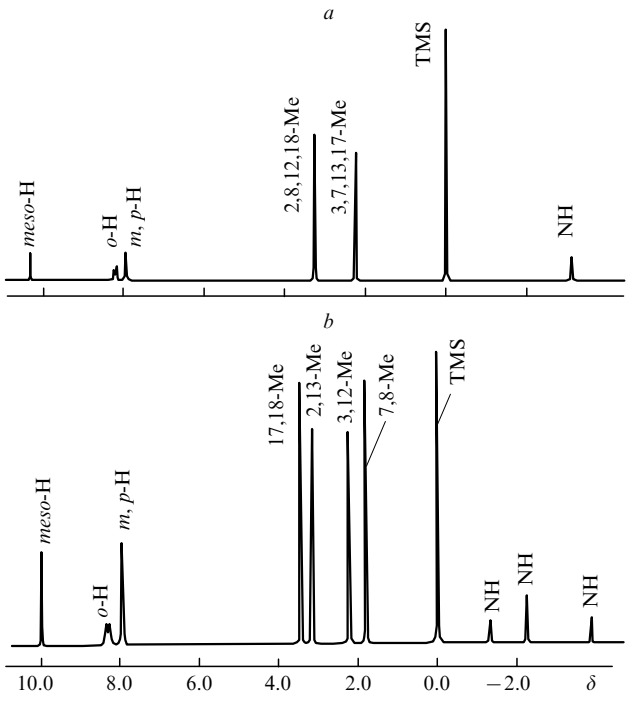


Figure 13. ^{1}H NMR spectra of 5,15-diphenyl-2,3,7,8,12,13,17,18-octamethylporphine (*a*) and 5,10-diphenyl-2,3,7,8,12,13,17,18-octamethylporphine (*b*) in $CDCl_3$ with 0.5% CF_3CO_2H.[55]
TMS is tetramethylsilane.

in deuteriochloroform at room temperature differs from that of the protonated porphyrin in the absence of the signals for the protons of the NH groups. Apparently, these peaks can be detected at lower temperatures. Other characteristics of the ^{1}H NMR spectra of protonated and non-protonated porphyrins are similar.

The ^{1}H NMR spectrum of the neutral form of porphyrin **17**, like that of compound **16**, does not contain signals corresponding to the protons of the NH groups; the latter appear upon protonation of the porphyrin at δ −2.47 and −1.26 (see Table 6 and Fig. 14). In the region of positive values of the chemical shifts, the ^{1}H NMR spectra of the neutral and protonated forms are virtually the same. Upon protonation, the signals of the protons of the methyl groups are shifted downfield by 0.04–0.13 ppm, while those of the *meso*-protons are shifted by 0.2 ppm.

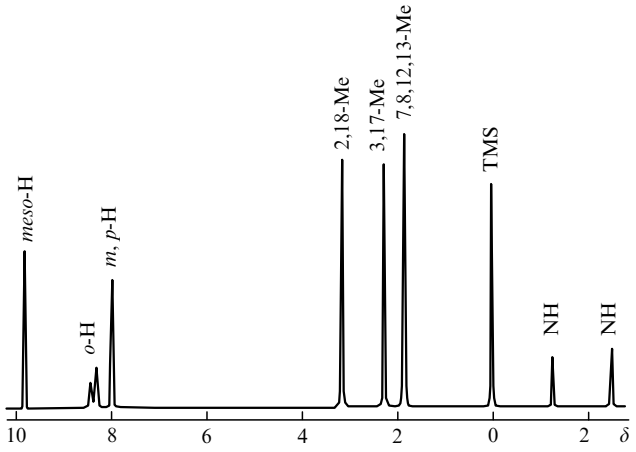


Figure 14. ^{1}H NMR spectrum of 5,10,15-triphenyl-β-octamethylporphine in $CDCl_3$ with 0.5% CF_3CO_2H.[55]

Steric repulsion of the phenyl and methyl substituents in the porphyrin **4** results in the saddle-shaped conformation of the macrocycle. In its ^{1}H NMR spectrum, this is manifested as a downfield shift of the signals for the protons corresponding to the NH groups and the appearance of a singlet at δ −1.14 . In addition, the ^{1}H NMR spectrum of the porphyrin **4** contains a singlet corresponding to the protons of the methyl groups at δ 1.84 and two multiplets corresponding to the *ortho*- (δ 8.35), *meta*- and *para*-protons (δ 7.93).

Analysis of the data listed in Table 6 suggests that the signals for the protons of the NH groups are gradually shifted downfield with an increase in the number of the phenyl substituents in the *meso*-positions of octamethylporphine. The signals for the *meso*-proton are shifted in the opposite direction in the same series. This suggests that the strength of the ring current decreases, while the degree of distortion of the porphyrin macrocycle increases in the following series of substituted octamethylporphines: unsubstituted < 5-phenyl- < 5,15-diphenyl- < 5,10-diphenyl- < 5,10,15-triphenyl- < tetraphenyloctamethylporphine.

A series of *meso*-phenyloctaethylporphine derivatives, *viz.*, 5-phenyl- (**18**), 5,15-diphenyl- (**19**), 5,10-diphenyl- (**20**), 5,10,15-triphenyl- (**21**) and 5,10,15,20-tetraphenyl-2,3,7,8,12,13,17,18-octaethylporphine (**3**), have been investigated.[56] The structures of these porphyrins were calculated using the semiempirical quantum-chemical method (PM3).

The results of optimisation of the structure of the monophenyl octaethylporphine derivative (**18**) by molecular mechanics methods (force field MM+) and PM3 (Fig. 15) are qualitatively similar, although the MM method predicts a somewhat larger deformation of the planar structure of the macrocycle. What is essential, is that the introduction of even one aryl substituent in the *meso*-position of a β-octaalkylporphine results in the distortion of its planar structure. The results of calculations of the structures of *meso*-phenyloctaethylporphine derivatives are shown in Fig. 16; the ^{1}H NMR spectra of porphyrins **3** and **18**–**21** are presented in Table 7.

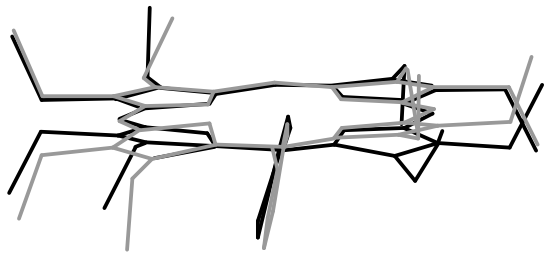


Figure 15. Structure of porphyrin **18** optimised using the MM (black coloured) and PM3 (grey coloured) methods.[56]

As expected, the simplest ^{1}H NMR spectrum was observed for β-octaethylporphine (**2**). This contains four signals: a singlet for the *meso*-proton (δ 10.10), a quartet (δ 4.11) and a triplet (δ 1.92) corresponding to the protons of the methyl and methylene groups and a singlet (δ −3.75) corresponding to the protons of the NH groups.

Introduction of a phenyl group into the *meso*-position of the macrocycle results in the complication of the ^{1}H NMR spectrum of the porphyrin **18** manifested in the appearance of additional signals for the protons of the phenyl substituent. Splitting of these signals is due to the anisotropic effect of the ring current of the macrocycle. The intensity of the magnetic field induced by this current diminishes the effect of an external magnetic field on the *ortho*-protons which are deshielded more strongly (δ 8.21) than the *meta*- and *para*-protons (δ 7.66 and 7.79, respectively). The signals of the ethyl groups adjacent to the benzene ring form a separate group as a result of anisotropic shielding by the phenyl substituent and are shifted upfield (δ 2.78 and 1.18) in comparison with the more remote ethyl groups (δ 4.12 and 1.89). The signals

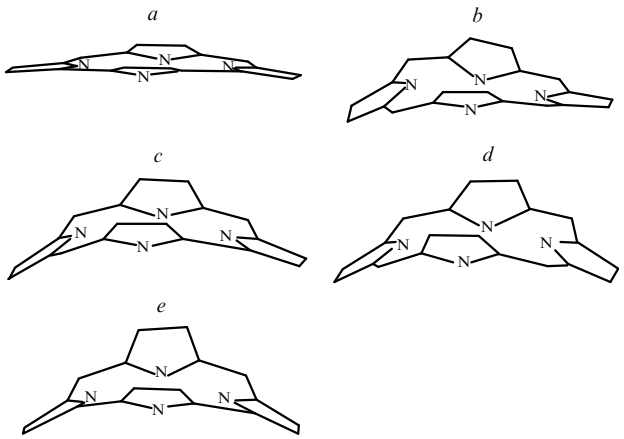


Figure 16. Structures of the tetrapyrrole cores of *meso*-phenyl derivatives of 2,3,7,8,12,13,17,18-octaethylporphin: H_2P (**19**) (*a*), H_2P (**20**) (*b*), H_2P (**21**) (*c*), H_2P (**3**) (*d*) and dodecaphenylporphine H_2P (**7**) (*e*) calculated using the PM3 method.[56]

Table 7. ^{1}H NMR spectra of octaethylporphine, its *meso*-phenyl derivatives and dodecaphenylporphine in $CDCl_3$ (hexamethyldisilane as an internal standard).[56]

Porphyrin	δ				
	meso-H	Ph		Et	NH
		o-H	*m*, *p*-H		
2	10.10, s	–	–	4.11, q; 1.92, t	−3.75, s
18	10.18, s; 9.93, s	8.21, d	7.79, d; 7.66, t	4.12, q; 1.89, t; 2.78, q; 1.18, t	−3.02, s; −3.15, s
19	10.23, s	8.21, d	7.78, d; 7.67, t	4.09, q; 1.89, t; 2.79, q; 1.18, t	−2.08, s
20	9.63, s	8.30, d	7.75, d; 7.67, t	3.92, q; 1.80, t; 3.80, q; 1.57, t; 2.65, q; 0.63, t; 2.25, q; 0.44, t	−2.72, br.s
21	9.45, s	8.32, m	7.71, m	3.75, q; 1.56, t; 2.70, q; 0.72, t; 2.25, m; 0.46, t; 0.37, t	−2.09, s
3	–	8.36, m	7.71, m	2.52, br.s; 0.47, br.s	–
7	–	8.02, m ; 7.06, m	6.69, m	–	−0.85, s

of the protons in the *meso*-positions and in the NH groups are split into two components, *viz*., δ 10.18, 9.93 and −3.02, −3.15, respectively. The fact that the signals of peripheral *meso*- and intracyclic NH group protons come closer suggests a decrease in the strength of the ring current of the macrocycle upon introduction of a *meso*-phenyl substitutent into the octaethylporphine molecule.

Diphenyl-β-octaethylporphine derivatives have a strongly distorted macrocycle, the distortion of the 5,15-substituted isomer **19** is much less pronounced than that of its non-symmetrical analogue **20** (see Fig. 16). The ^{1}H NMR spectra of these compounds manifest a downfield shift of the signals for the protons of the NH groups to δ −2.08 (for the symmetrical isomer **19**) and to δ −2.72 (for the 5,10-substituted analogue **20**). Special mention should be made of a significant broadening of the signals for the protons of the NH groups in the ^{1}H NMR spectrum of the porphyrin **20**.

The signals for the *meso*-protons of the porphyrin **19** are present at δ 10.23 and are slightly shifted downfield in comparison with the corresponding signals in the ^{1}H NMR spectrum of compound **18**. At the same time, the signals for the *meso*-protons in the ^{1}H NMR spectrum of the porphyrin **20** are shifted noticeably upfield (δ 9.63).

The signals for the *meta*- and *para*-protons of the *meso*-phenyl groups in the ^{1}H NMR spectra of compounds **19** and **20** do not change their positions relative to the corresponding signals in the ^{1}H NMR spectrum of the porphyrin **18**. A noticeable shift of the signals for the *ortho*-protons of the phenyl groups of the non-symmetrical isomer **20** can be attributed to the effect of steric factors. The phenyl rings of the more strongly distorted porphyrin **20** cannot any longer be perpendicular to the plane of the macrocycle and are rotated relative to the framework of the molecule. As a result, the *ortho*-protons of the phenyl substituents that are close to the macrocycle are exposed to the stronger deshielding effect of the ring current of the porphyrin as a result of which their signals are shifted downfield (δ 8.30).

An analogous trend for the signals of the protons of the NH groups and the protons in the *meso*-positions to come closer to each other can also be traced in the ^{1}H NMR spectrum of triphenyloctaethylporphine **21**: the degree of the distortion of the macrocycle increases with an increase in the number of peripheral substituents.

The results of quantum-chemical calculations and ^{1}H NMR spectroscopic data suggest that dodecaphenylporphine (**7**) is distorted to the greatest extent. The protons of the NH groups in its ^{1}H NMR spectrum resonate in the lowest field, at δ −0.85. The protons in the *meta*- and *para*-positions of the *meso*- and β-phenyl substituents are not resolved and appear as a multiplet at δ 6.69. The signals for the *ortho*-protons of the phenyl groups in the β-positions are observed at δ 7.06, while those in the *meso*-positions are observed at δ 8.02.

Analysis of ^{1}H NMR spectroscopic data revealed that the introduction of the phenyl substituents in the *meso*-positions of β-octaethylporphine causes distortion of the aromatic tetrapyrrole core which increases in the following order: **2** < **18** < **19** < **20** < **21** < **3** < **7**.

Porphyrins containing from 8 to 12 phenyl substituents have been synthesised and their ^{1}H NMR spectra have been analysed.[31] The strength of the ring current of the macrocycle decreases with an increase in the number of peripheral substituents (Table 8). One of two decaphenyl porphine derivatives, *viz*., the non-symmetrical *cis*-isomer, manifests a higher degree of distortion than the 5,15-substituted *trans*-analogue.

Table 8. ^{1}H NMR spectra of phenyl-substituted porphyrins in $CDCl_3$ (TMS as an internal standard).[31]

Porphyrin	δ	
	NH	*meso*-H
β-Octakis(4-isopropylphenyl)porphine	−3.03	10.32
trans-Decaphenylporphine	−2.06	10.15
cis-Decaphenylporphine	−2.0	9.92
Undecaphenylporphine	−1.10	9.63
Dodecaphenylporphine	−0.90	–

The dynamics of conformational changes in spatially distorted porphyrins in solution was monitored by following the temperature dependence in the ^{1}H NMR spectra.[24, 25, 27, 57, 58] At 298 K, dodecaphenylporphine (**7**) gives three low-field signals corresponding to the protons of the phenyl groups (Fig. 17). Splitting of two multiplet signals at δ 6.5–7 into two triplets is observed at temperatures below 253 K; the doublet at δ ~7.6 corresponding to the *ortho*-protons of the *meso*-phenyl rings undergoes splitting at temperatures below 243 K. At 193 K, the ^{1}H NMR spectrum contains six doublets and nine triplets with the integral intensities of unity each. Similar temperature-dependent changes are observed in the ^{1}H NMR spectrum of the dication H_4P (**7**)$^{2+}$. An unusually broad range of chemical shifts of the signals for the *ortho*-protons of the β-phenyl rings of dodecaphe-

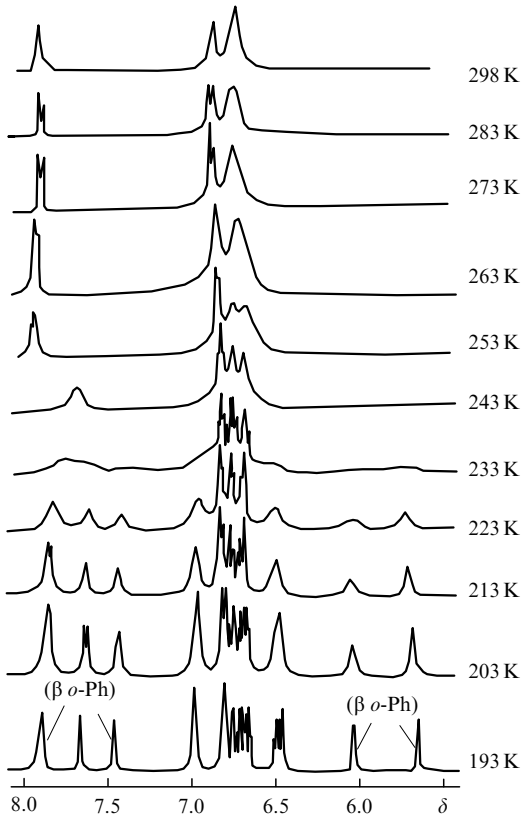


Figure 17. Temperature dependence of the ^{1}H NMR spectrum of dodecaphenylporphine in CD_2Cl_2.[25]

nylporphine and its protonated form at low temperatures was attributed[25] to different positions of these protons relative to the macrocyclic core and, correspondingly, to different effects of the ring current on these protons. The *ortho*-protons of the β-phenyl group deviate from the mean plane of the porphyrin skeleton to a larger distance and are shielded to a lesser degree in comparison with aromatic ring protons less deviated from the plane.

Analysis of the temperature dependence of the ^{1}H NMR spectrum of the porphyrin **7** revealed that its molecules take part in two dynamic processes. One of them is NH-tautomerism.[58] The value of the Gibbs activation energy, $\Delta G^{\neq}$, calculated for this reaction is 54 kJ mol^{-1} (see Ref. 25), *i.e.*, is commensurate with the corresponding values for planar tetraarylporphyrins.[49] The second dynamic process, which is more characteristic of distorted porphyrins,[19,29] entails inversion of the macrocycle. The $\Delta G^{\neq}$ value of this process for the porphyrin **7** is ~46 kJ mol^{-1} (see Ref. 25). Only one dynamic process, *viz.*, inversion of the macrocycle ($\Delta G^{\neq} = 45.5$ kJ mol^{-1}), is observed for the dication $H_4P(7)^{2+}$. It is noteworthy, however, that no dynamic processes take place in the case of the nickel dodecaphenylporphine complex ($\Delta G^{\neq} < 30$ kJ mol^{-1}) despite the same degree of distortion of the molecule. Presumably, the barrier to inversion of the macrocycle in the complex NiP (**7**) is too low to be recorded. This is consistent with the data for nickel complexes of octamethyl-, octaethyl- and octapropyltetraphenylporphines where the barriers to inversion of the macrocycles are much lower than those in the corresponding free bases and their dications.[24]

Distortion of the porphyrin core also manifests itself in the Raman spectra.[59–61] The frequency range (1300–1700 cm^{-1}) of porphyrin complexes, which comprises a series of structure-sensitive 'marker' lines ($\nu_2-\nu_4$) corresponding to the stretching of the $C_\alpha-N$ (ν_2), $C_\alpha-C_{ms}$ (ν_3) and $C_\beta-C_\beta$ (ν_4) bonds, is the most interesting and informative one.[61] Analysis of a series of distorted nickel complexes of octaalkyltetraphenylporphines and planar complexes of octaalkylporphines has shown[60] that in the former case the 'marker' line frequencies in the Raman spectra increase with an increase in the size of the coordination cavity. Contrariwise, in the case of octaalkylporphine complexes an increase in the size of the coordination cavity results in a shift of the structure-sensitive lines ν_2, ν_3 and ν_4 towards the lower frequencies. Based on the data obtained, the lines $\nu_2-\nu_4$ were termed as 'core-size marker lines'. The Raman spectra of a series of distorted porphyrin **3** complexes with Ni, Co, Cu and Zn have been analysed.[16] A correlation between the size of the central cavity and the frequency of the bands $\nu_2-\nu_4$ was opposite to the dependence established[60] for a series of nickel complexes of β-octaalkyl-*meso*-tetraphenylporphines. The size of the coordination cavity is determined by both the deviation of the porphyrin core from planarity as a result of introduction of peripheral substituents and the size of the metal cation; however, the contribution of each of these factors is different.

It was found[16] that the size of the central cavity is not a crucial factor in determining the position of the 'marker' lines. The angle $C_\alpha-N-C_\alpha$ is yet another parameter that influences the frequency of these marker lines. The lines ν_2, ν_3 and ν_4 are always shifted towards the lower frequencies with an increase in the angle $C_\alpha-N-C_\alpha$. Apparently, the magnitude of this angle is closely related to the vibration frequencies of the bonds contributing to the 'marker' lines.

The frequencies of the 'marker lines' in solution and in the crystalline states differ insignificantly, which suggests the similarity of the conformations of the macrocycle both in solution and in the crystal (Table 9).

Distortion of the tetrapyrrole core is manifested specifically in the electronic absorption spectra. The electronic absorption spectra of some *meso*-phenyloctamethylporphine derivatives in acetic acid are shown in Fig. 18.[55] With an increase in the degree of distortion of the porphyrin macrocycle, all absorption bands manifest bathochromic shifts. These spectral changes are so characteristic that the red shift of all electronic absorption spectra bands can be reliably interpreted as the deformation of the tetrapyrrole macrocycle.[8]

The data from the electronic absorption spectra of octaethylporphine, its *meso*-phenyl derivatives and dodecaphenylporphine are listed in Table 10. As can be seen, the absorption maxima of the porphyrins are shifted regularly towards the red region with an increase in the degree of extraplanar distortion of the macrocycle irrespective of the solvent used. The reason for these spectral

Table 9. 'Marker' vibration frequencies of β-octaethyl-*meso*-tetraphenylporphine complexes (**3**) in CS_2 and in the crystalline state.[16]

Complex	ν_4 /cm^{-1}		ν_3 /cm^{-1}		ν_2 /cm^{-1}		ν_ϕ /cm^{-1}	
	for solution in CS_2	for crystal	for solution in CS_2	for crystal	for solution in CS_2	for crystal	for solution in CS_2	for crystal
NiP (**3**)	1360	1360	1504	1506	1563	1565	1598	1599
CoP (**3**)	1354	1356	1500	1506	1560	1558	1597	1599
CuP (**3**)	1354	1356	1503	1503	1556	1557	1596	1598
ZnP (**3**) · MeOH	1348	–	1495	–	1548	–	1594	–

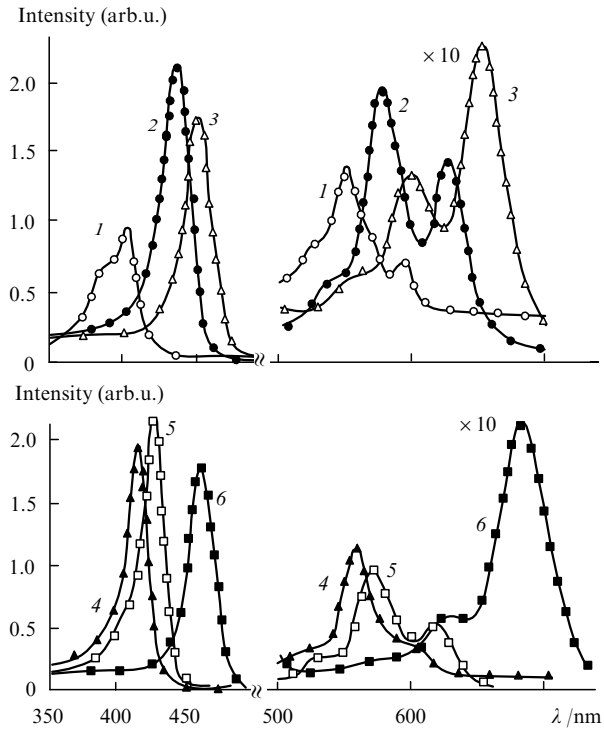


Figure 18. Electronic absorption spectra of β-octamethylporphine (*1*) and its *meso*-phenyl derivatives: 5,10-diphenyl- (*2*), 5,10,15-triphenyl- (*3*), 5-phenyl- (*4*), 5,15-diphenyl- (*5*) and 5,10,15,20-tetraphenyl-2,3,7,8,12,13,17,18-octamethylporphine (*6*) in acetic acid.[55]
The intensities of the bands in the visible region of the spectrum are increased 10-fold.

changes is the deformation of the macrocycle, which reduces its aromaticity.

The ruffled and saddle conformations of zinc complexes of unsubstituted porphine (**22**) and *meso*-tetrakis(trifluoromethyl)-porphine (**23**) were optimised using the density functional theory-based analysis of configuration interaction calculations with single excitations (DFT/SCI).[62, 63] An artificial distortion of the macrocycle of the zinc porphine complex was performed in order to prove the appearance of a bathochromic shift in the absorption spectra in the absence of electronic effects of substituents. The distorted skeleton of ZnP (**23**) with all the *meso*-CF_3 groups replaced by hydrogen atoms was used to derive a ruffled conformation of ZnP (**22**). A similar approach was used to derive a saddle conformation of ZnP (**22**) based on β-octamethyl-*meso*-tetraphenylporphine.

The results of DFT/SCI computations (Tables 11 and 12) provide an adequate description of excited states of different types of porphyrins.[62, 64, 65] As can be seen from Table 12, the *Q*-bands of the non-planar conformations of ZnP (**23**), *viz*., the ruffled conformation at 582 nm and the saddle conformation at 576 nm, are shifted bathochromically relative to the *Q*-band of the planar conformation of ZnP (**22**) (by 24 and 18 nm, respectively), which is consistent with the experimental data.[66, 67] The calculated data on simulated distortions of the ZnP (**22**) macrocycle also predicted a long-wavelength shift of the bands in the electronic adsorption spectra of the ruffled and saddle conformations (by 17 and 27 nm, respectively). The *B*-bands in all distorted porphyrins are shifted towards the red region, apparently as a result of destabilisation of their upper occupied orbitals.

Semiempirical quantum-chemical calculations of saddle, ruffled and dome-like conformations of a magnesium porphine complex [68] gave similar results, *viz*., with an increase in the degree of distortion of the planar structure of the porphyrin core, all absorption bands manifested a bathochromic shift due to the advanced destabilisation of the HOMO.

The results of spectroelectrochemical [69, 70] and electrochemical measurements [70–75] provide additional experimental evidence in favour of stronger destabilisation of the HOMO upon deformation of the macrocycle than the LUMO. The redox potentials of zinc complexes of tetrakis(pentafluorophenyl)porphine (**24**) and its octabromo- (**25**), octachloro- (**26**) and octamethyl- (**27**) derivatives are listed in Table 13. As can be seen, the octachloro and octabromo derivatives are reduced more easily (by 0.48 and 0.47 V, respectively) and are oxidised less easily (by 0.26 and 0.20 V, respectively) than the planar complex ZnP (**24**). Hence, the energy gap between the bonding and antibonding orbitals

Table 10. Electronic absorption spectra of octaethylporphine, its *meso*-phenyl derivatives and dodecaphenylporphine.[56]

Porphyrin	Solvent	Absorption band maxima λ_{max} /nm (log ε)				
		I	II	III	IV	Soret
2	$CHCl_3$	620 (3.74)	568 (3.86)	535 (4.04)	499 (4.15)	400 (5.25)
	pyridine	620	567	531	497	389
	AcOH	592		551		400
18	$CHCl_3$	624 (3.54)	573 (3.90)	538 (3.97)	505 (4.24)	405 (5.31)
	pyridine	626 sh	572	535	502	405
	AcOH			560		413
19	$CHCl_3$	627 (3.30)	575 (3.87)	542 (3.76)	508 (4.25)	410 (5.35)
	pyridine	627	575	538	506	409
	AcOH	621		574		430
20	$CHCl_3$	sh	578 (3.89)	sh	510 (4.25)	413 (5.39)
	pyridine	sh	593	sh	518	420
	AcOH	633		583		437
21	$CHCl_3$	667 (3.79)	608 (3.91)	sh	534 (4.14)	438 (5.28)
	pyridine	679	613	570	533	432
	AcOH	661		608		456
3	$CHCl_3$ + 0.5% NEt_3	696 (3.75)	598 (3.82)	sh	551 (4.14)	452 (5.34)
	pyridine	698	592	sh	548	456
	AcOH	688		633		467
7	$CHCl_3$	717 (4.02)	–	612 (4.13)	561 (4.17)	465 (5.34)
	pyridine	742	–	636	569	491
	AcOH	722		–		492

Table 11. Energies of highest occupied and lowest unoccupied molecular orbitals of porphyrin metallocomplexes.[64]

Complex (symmetry)	Energy of orbitals /eV					
	LUMO + 2	LUMO + 1	LUMO	HOMO	HOMO − 1	HOMO − 2
ZnP (**22**) (D_{4h})	−0.73 (a_{1u})	−2.31 (e_g)	−2.31 (e_g)	−5.33 (a_{2u})	−5.39 (a_{1u})	−6.59 (a_{1g})
ZnP (**22**) (ruffled D_{2h})	−0.81 (a_1)	−2.33 (e)	−2.33 (e)	−5.30 (b_2)	−5.34 (b_1)	−6.51 (nb_1) [a]
ZnP (**23**) (ruffled D_{2h})	−1.93 (a_1)	−3.45 (e)	−3.45 (e)	−6.23 (b_1)	−6.52 (b_2)	−7.47 (nb_1) [a]
ZnP (**22**) (saddle D_{2h})	−0.85 (a_1)	−2.35 (e)	−2.35 (e)	−5.26 (b_2)	−5.34 (b_1)	−6.68 (nb_2) [a]
ZnP (**23**) (saddle C_{2v})	−1.86 (a_1)	−3.31 (b_2)	−3.43 (b_1)	−6.22 (a_2)	−6.53 (a_1)	−7.48 (na_1) [a]

[a] n is the second highest occupied molecular orbital of the given symmetry.

Table 12. Symmetry (S) and energies (ΔE) of transitions and oscillator strengths (f) of model metalloporphyrins.[62, 65]

Complex, conformation	Absorption bands	S	ΔE /eV (λ /nm)	f	Main contributions			
ZnP (**22**)	Q	E_u	2.22 (558)	0.002	50% ($a_{2u}-e_g$)	49% ($a_{1u}-e_g$)		
	B	E_u	3.92 (316)	1.729	38% ($a_{2u}-e_g$)	42% ($a_{1u}-e_g$)		
ZnP (**22**),	Q	E	2.16 (575)	0.003	49% (b_2-e)	50% (b_1-e)		
ruffled	B	E	3.82 (325)	0.821	20% (b_2-e)	21% (b_1-e)	51% (nb_1-e) [a]	
ZnP (**23**),	Q	E	2.13 (582)	0.012	44% (b_2-e)	54% (b_1-e)		
ruffled	B	E	3.72 (333)	0.223	6% (b_2-e)	5% (b_1-e)	85% (nb_1-e) [a]	
ZnP (**22**),	Q	E	2.12 (585)	0.002	50% (b_1-e)	49% (b_2-e)		
saddle	B	E	3.74 (332)	1.403	51% (b_1-e)	48% (b_2-e)		
ZnP (**23**),	Q_x	B_2	2.14 (578)	0.013	44% (a_1-b_2)	55% (a_2-b_1)		
saddle	Q_y	B_1	2.15 (576)	0.012	54% (a_2-b_2)	44% (a_1-b_1)		
	B_y	B_1	3.78 (328)	1.164	27% (a_2-b_2)	29% (a_1-b_1)	16% (na_1-b_1) [a]	14% ($2na_1-b_1$) [a]
	B_x	B_2	3.79 (327)	1.370	31% (a_1-b_2)	35% (a_2-b_1)	14% (na_1-b_2) [a]	10% ($2na_1-b_2$) [a]

[a] n and $2n$ are the second and third highest occupied molecular orbitals of the given symmetry.

Table 13. Redox potentials of zinc complexes of porphyrins (V).[69, 70]

Complex	$E^\circ_{2+/0}$	$E^\circ_{2+/1+}$	$E^\circ_{1+/0}$	$E^\circ_{0/1-}$	$E^\circ_{1-/2-}$
ZnP (**1**)	–	1.16	0.80	−1.33	−1.66
ZnP (**24**)	–	1.58	1.37	−0.95	−1.37
ZnP (**25**)	1.55	1.53	1.57	−0.48	−0.76
ZnP (**26**)	1.60	1.57	1.63	−0.47	−0.75
ZnP (**27**)	0.98	0.99	0.97	−1.14	−1.52

Note. The potentials were measured using a reference chloride electrode in 1.0 M KCl; $Fc_{1+/0}$ = 0.48 V; 0.1 M $[NBu_4]^+[PF_6]^-/CH_2Cl_2$.

diminishes upon distortion of the porphyrin macrocycle. When analysing the data presented in Table 13, account must be taken of the fact that, unlike the phenyl groups, pentafluorophenyl substituents and halogen atoms possess electron-withdrawing properties and thus make a greater contribution to the stabilisation of the HOMO and LUMO of ZnP (**25**) and ZnP (**26**) complexes in comparison with ZnP (**24**).

Zinc complexes of 2,3,12,13-tetrasubstituted 5,10,15,20-tetraphenylporphines, which contain trifluoromethyl (**28**) and methyl (**29**) substituents and bromine atoms (**30**), have been synthesised.[75] The structures of the complexes (as crystal solvates) of ZnP (**28**)·$(EtOH)_3$, ZnP (**29**)·$(THF)_{1.6}$·$(CHCl_3)_{0.4}$ and ZnP (**30**)·MeOH·DMF have been established. Their macrocycles have a saddle, slightly ruffled conformation; the structure of the porphyrin containing trifluoromethyl groups is deformed to the greatest extent (Fig. 19). Presumably, this deformation is due to the square-pyramidal coordination of the zinc cation rather than to the steric repulsion of the peripheral substituents. These structural data can be correlated to spectral and electrochemical characteristics.

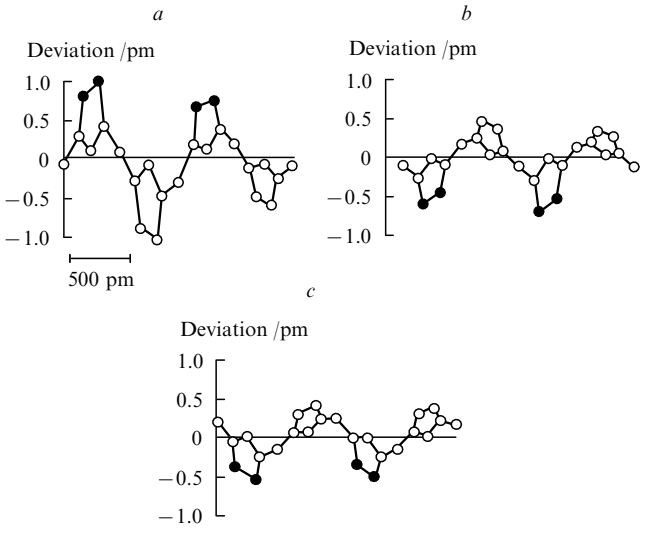


Figure 19. Deviations of the atoms in the macrocycles of zinc complexes of porphyrins **28** (*a*), **29** (*b*) and **30** (*c*) from the mean plane passing through four nitrogen atoms.[75] The positions of the substituents are coloured black.

All absorption bands in the electronic spectrum of ZnP (**28**) are shifted bathochromically in comparison with the electronic spectra of ZnP (**29**) and ZnP (**30**) (Fig. 20). Cyclic voltammetric studies of the redox properties of zinc complexes of porphyrins (**28**–**30**) revealed that their oxidation and reduction potentials increase with an enhancement of the electron-withdrawing properties of the substituents, these dependences being nearly linear for the oxidation and S-shaped for the reduction (Fig. 21). The

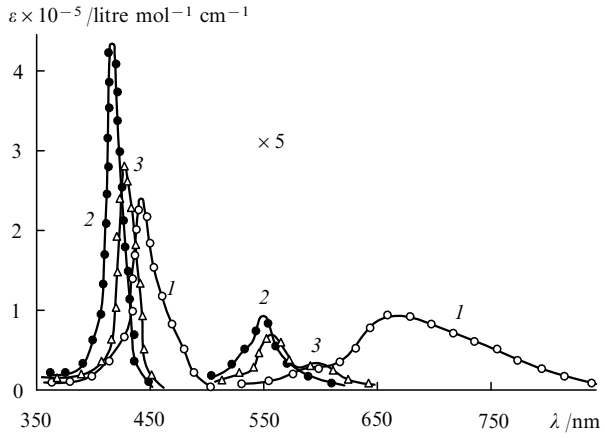


Figure 20. Electronic absorption spectra of zinc complexes of 2,3,12,13-tetrasubstituted derivatives of tetraphenylporphine ZnP (**28**) (*1*), ZnP (**29**) (*2*) and ZnP (**30**) (*3*) in $C_2H_4Cl_2$. The intensities of the bands in the visible region of the spectrum are increased 5-fold.[75]

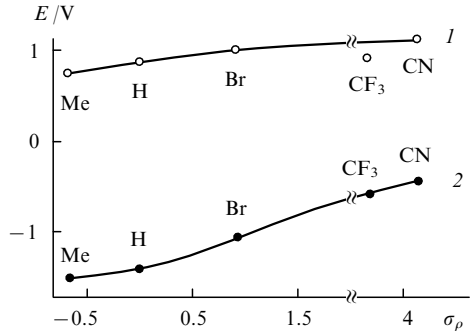
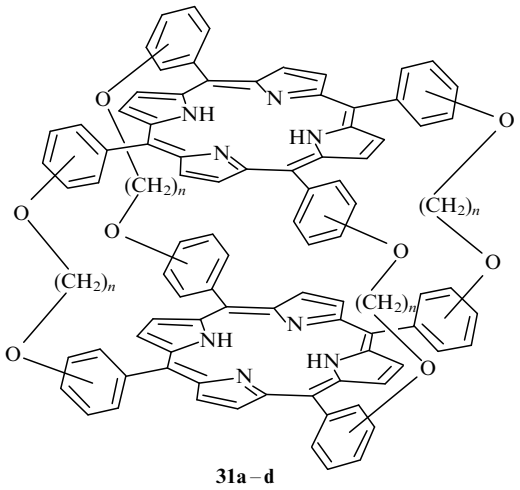


Figure 21. Dependences of the first oxidation (*1*) and reduction (*2*) potentials of zinc complexes of tetrasubstituted tetraphenylporphine derivatives measured in $C_2H_4Cl_2$ *vs.* a saturated calomel electrode on the values of the Hammett constants σ_ρ of substituents.[75]



31a–d

m-bridge, $n = 4$ (**a**), *m*-bridge, $n = 3$ (**b**), *m*-bridge, $n = 2$ (**c**), *o*-bridge, $n = 3$ (**d**).

difference between the oxidation and reduction potentials decreases with an enhancement of the electron-withdrawing properties of the substituents, the destabilisation of the HOMO being greater than that of the LUMO. The difference between the orbital energies for ZnP (**1**) is 2.2 V, whereas that for its trifluoromethyl derivative is as small as 1.5 V. Thus, the energies of the MO of porphyrins and their redox characteristics strongly depend on spatial distortion of their central core and the electronic nature of substituents.

IV. Coordination properties

The effect of the distortion of the planar structure of a macrocycle on the coordination properties of porphyrins was observed for *N*-substituted derivatives.[76] However, one can hardly distinguish structural changes in the coordination centre of the macrocycle due to substitution from the distortion of the macrocycle itself. The effect of distortion as such on the coordination properties was established in the analysis of the dimeric tetraphenylporphine derivatives **31a–d** where the monomeric fragments are linked through benzene nuclei by four bridges of the type $O(CH_2)_nO$, $n = 2–4$.[77–83]

For steric reasons, all C–C bonds of the bridging groups of the cyclophane dimer **31a** cannot adopt *trans*-configurations. The energy required for transition from the transoid configuration of one of these bonds to the gauche configuration is less than 4 kJ mol^{-1}. The overall change in the configuration of one bond in each of the four bridges suffices for the disturbance of the planar structure of the tetrapyrrole cores in the dimer **31a**.[77] Studies on the kinetics of formation and dissociation of complexes of the dimers **31a–d** containing bridging groups of various lengths have shown [78–83] that the reactivities of these porphyrins increase by a factor of tens of thousands as a result of spatial distortion of their macrocycles. Considering that the acid–base and coordination properties of porphyrins are closely interrelated,[90] it is not surprising that spatially distorted porphyrins significantly exceed their planar counterparts in basicities.[84–89] Stretching and polarisation of the N–H bonds in the transition state of a reacting system 'a metal solvatocomplex–porphyrin' make a significant contribution to the energy of complex formation. At the same time, strong interactions of metal cations with tertiary nitrogen atoms of porphyrin occur in the transition state, which decrease both the energy of the transition state and the activation energy of the reaction. Thus, an increase in the electron density on the nitrogen atoms not only provides easier access to them due to the deformation of the macrocycle, but also increases appreciably the rate of formation of metalloporphyrins. This is confirmed by kinetic data on coordination of octamethylporphine, octaethylporphine and their phenyl derivatives by copper and zinc ions in pyridine and DMF (Tables 14 and 15).

The equation of complexation can be presented as follows:

$$H_2P + MX_2 \longrightarrow MP + 2HX.$$

The kinetic order of this reaction with respect to porphyrin for all the porphyrins described in this review is equal to unity. With respect to metal salts, the situation is more complicated, *viz.*, the kinetic order of the reaction depends on the degree of ionisation of the solvatocomplex in solution.[91]

The data presented in Tables 14 and 15 suggest that the complexation rates of phenyl derivatives of octamethyl- and octaethylporphine in pyridine and DMF increase with an increase in the number of peripheral substituents, 5,10-diphenyl derivatives reacting at much faster rates than their 5,15-substituted analogues. The reaction rate increases 3–4 orders of magnitude, while the activation energy decreases 2–2.5-fold on going from planar octaalkylporphines to the most deformed tetraphenyl derivatives. Introduction of eight β-alkyl substituents on going from porphine to etioporphyrin and of four *meso*-phenyl groups on going from porphine to tetraphenylporphine causes only a 7-fold increase in the complexation rate. In other words, the drastic increase in the complexation rates resulting from the introduction of *meso*-aryl substituents into β-octaalkylporphines

Table 14. Rate (k), energy of activation (E) and changes in the entropy of activation ($\Delta S^{\neq}$) of the coordination of octamethylporphine (**13**) and its phenyl derivatives by copper and zinc ions in pyridine.[55]

Porphyrin	Copper acetate			Zinc acetate		
	$k^{298} \times 10^4$ /litre$^{0.4}$ mol$^{-0.4}$ s^{-1}	E /kJ mol^{-1}	$\Delta S^{\neq}$ /J (mol K)$^{-1}$	$k^{328} \times 10^4$ /litre mol^{-1} s^{-1}	E /kJ mol^{-1}	$\Delta S^{\neq}$ /J (mol K)$^{-1}$
13	0.01	153.9 ± 0.7	148 ± 2	20.2 ± 0.4	102.8 ± 1.0	9 ± 3
14	0.31	93.4 ± 0.3	-25 ± 1	31.7 ± 0.8	70.6 ± 0.7	-86 ± 2
15	5.46	85.1 ± 0.6	-30 ± 2	40.9 ± 0.1	64.2 ± 0.5	-103 ± 2
16	10.1 ± 0.1	85.0 ± 1.1	-25 ± 4	754 ± 1.5	56.6 ± 1.7	-101 ± 5
17	105 ± 2	77.3 ± 0.9	-31 ± 3	2860 ± 3	54.6 ± 0.4	-97 ± 1
4	116 ± 1	67.9 ± 1.4	-70 ± 4	37310 ± 13	47.0 ± 0.9	-118 ± 3

Table 15. Kinetic parameters of coordination of octaethylporphine (**2**), its phenyl derivatives and dodecaphenylporphine (**7**) by copper ions upon treatment with copper(II) acetate in DMF and pyridine.[56]

Porphyrin	Pyridine			DMF		
	$k_{1.4}^{298} \times 10^4$ /litre$^{0.4}$ mol$^{-0.4}$ s^{-1}	E /kJ mol^{-1}	$\Delta S^{\neq}$ /J (mol K)$^{-1}$	$k_{n+1}^{328} \times 10^4$ /litre$^{0.5}$ mol$^{-0.5}$ s^{-1}	E /kJ mol^{-1}	$\Delta S^{\neq}$ /J (mol K)$^{-1}$
2	very slow			34 ± 2	95 ± 1	19 ± 3
18	0.46 ± 0.02	68 ± 1	-108 ± 3	452 ± 40	88 ± 1	17 ± 3
19	0.29 ± 0.01	103 ± 2	6 ± 5	248 ± 10	57 ± 2	-92 ± 5
20	7.14 ± 0.2	94.2 ± 0.2	3 ± 5	–	–	–
21	38.71 ± 0.6	96 ± 0.8	23.1 ± 4	–	–	–
3	1502 ± 40	61 ± 1	-64 ± 3	5657 ± 200	28 ± 1	-164 ± 3
7	919 ± 20	21 ± 1	-202 ± 3	very fast		

cannot be due to the electronic effects of the substituents alone and is caused primarily by the changes in the geometry of the porphyrin molecules. Additional evidence in favour of this idea comes from the changes [more than 100 J (mol K)$^{-1}$] in the entropy of activation of the complexation for the porphyrins under study. These structural changes influence indirectly the electronic structure of the macrocycle by decreasing its aromaticity and increasing the electron density on the nitrogen atoms in the coordination centres of porphyrins.

The changes in the reactivities of phenyl-substituted β-octaalkylporphines in acetic acid are different in principle (Tables 16 and 17). With an increase in the number of phenyl substituents, the rate of complex formation decreases $\sim 10^4$-fold. In acetic acid, no dodecaphenylporphine complexes are formed at all. The activation energy of this reaction increases threefold on going from octaalkylporphines to their tetraphenyl derivatives, whereas the changes in the entropy of activation exceed 100 J (mol K)$^{-1}$. This can be attributed to the fact that the basicities of porphyrins increase with the degree of distortion of the tetrapyrrole macrocycles as a result of which tertiary nitrogen atoms acquire an ability to form more stable hydrogen bonds with acetic acid molecules blocking the coordination centre. Thus, the dicationic form generated by dodecaphenylporphine in acetic acid is inert with respect to coordination by transition metal ions.

The dissociation kinetics of copper(II), cobalt(II) and manganese(III) complexes with spatially distorted porphyrins in mixtures of acetic and trifluoroacetic acids has been studied (Table 18).[56, 92, 93] The kinetic order of this reaction with respect to metalloporphyrin and trifluoroacetic acid is equal to unity, which suggests a two-step dissociation mechanism [94] according to which the first M–N bond of the metalloporphyrin is cleaved under the action of a strong proton donor, *e.g.*, $MeCO_2H_2^+$, formed upon protonation of the oxygen atom of acetic acid, while the second bond is cleaved by a relatively weak acetic acid present in the system in a large excess. This activation barrier is overcome upon cleavage of the second M–N bond.

As can be seen from Table 18, the dissociation rates of copper and cobalt complexes of porphyrins increase, while the energies of activation decrease with an increase in the degree of distortion of the aromatic tetrapyrrole core. Introduction of the first two *meso*-phenyl substituents affects the kinetic parameters of this reaction to a far lesser degree than the introduction of the next two substituents. Dodecaphenylporphine complexes dissociate upon dissolution in acetic acid in the absence of sulfuric or trifluoro-

Table 16. Kinetic parameters of coordination of octamethylporphine and its phenyl derivatives by copper and zinc ions in acetic acid.[55]

Porphyrin	Copper acetate			Zinc acetate		
	$k^{298} \times 10^4$ /litre$^{0.5}$ mol$^{-0.5}$ s^{-1}	E /kJ mol^{-1}	$\Delta S^{\neq}$ /J (mol K)$^{-1}$	$k^{328} \times 10^4$ /litre mol^{-1} s^{-1}	E /kJ mol^{-1}	$\Delta S^{\neq}$ /J (mol K)$^{-1}$
13	3676 ± 4	28.3 ± 1.1	-166 ± 3	280 ± 1	39.2 ± 0.9	-163 ± 3
14	578 ± 1	55.3 ± 0.8	-91 ± 3	102 ± 1	45.7 ± 0.6	-152 ± 2
15	470 ± 1	71.2 ± 1.1	-39 ± 4	71.0 ± 0.1	70.9 ± 0.1	-77.8 ± 0.3
16	8 ± 1	72.4 ± 1.6	-36 ± 5	60.0 ± 0.1	78.8 ± 0.7	55 ± 2
17	5.70 ± 0.02	76.8 ± 0.7	-57 ± 2	very slow		
	0.34 ± 0.01	111.6 ± 0.6	36 ± 2	no reaction		

Table 17. Kinetic parameters of coordination of β-octaethylporphine, its *meso*-phenyl derivatives and dodecaphenylporphine by copper ions upon treatment with copper(II) acetate in acetic acid.[92]

Porphyrin	$k_{1.5}^{298}$ /litre mol^{-1} s^{-1}	E /kJ mol^{-1}	$\Delta S^{\neq}$ /J (mol K)$^{-1}$
2	1.66 ± 0.03	31.2 ± 0.3	−144 ± 1
18	0.53 ± 0.01	73.0 ± 0.4	−13.3 ± 1.5
19	0.180 ± 0.005	65 ± 2	−49.1 ± 2
3	0.00021 ± 0.00001	44.4 ± 1	−174 ± 2
7	complex is not formed		

Table 18. Kinetic parameters of dissociation of copper, cobalt and manganese complexes of octaethylporphine and its *meso*-phenyl derivatives in acetic acid with 0.069 M CF_3CO_2H.[56, 93]

Complex	$k^{298} \times 10^4$ /litre mol^{-1} s^{-1}	E /kJ mol^{-1}	$\Delta S^{\neq}$ /J (mol K)$^{-1}$
CuP (**2**)	0.668	99.3 ± 0.5	0.5 ± 1.5
CuP (**18**)	1.24	81.8 ± 0.7	−53 ± 2
CuP (**19**)	2.27	61.3 ± 0.6	−117 ± 2
CuP (**3**)	1030	46.3 ± 1	−140 ± 3
CoP (**2**)	0.787	69.5 ± 0.7	−98 ± 2
CoP (**18**)	5.43	57.7 ± 1.3	−122 ± 4
CoP (**19**)	14.5	46.6 ± 0.4	−151 ± 2
CoP (**3**)	954	15.7 ± 0.7	−220 ± 2
MnP (**2**)	–	–	–
MnP (**18**)	0.0249	26.9 ± 0.6	−270 ± 5
MnP (**19**)	0.480	27.4 ± 0.3	−244 ± 6
MnP (**3**)	8.01	38.5 ± 0.3	−183 ± 3

acetic acid. Apparently, the greater the distortion of the starting porphyrin the stronger are the strains of the coordination bonds M—N and the higher is the effective negative charge on the nitrogen atoms exposed to the electrophilic attack by the solvated proton.

The entropies of activation of the dissociation of copper and cobalt porphyrin complexes decrease regularly with an increase in the number of phenyl substituents, which suggests an increase in the degree of ordering of the 'metalloporphyrin – solvated proton' system in the transition state. The energies and entropies of the activation in the dissociation of cobalt complexes are significantly lower in comparison with the copper analogues. This correlates with the properties of Cu(II) and Co(II) cations: the formation of square-planar complexes is more characteristic of the former, whereas the latter largely produce octahedral complexes. Obviously, in the transition state the cobalt cation leaving the coordination centre of the porphyrin is solvated more efficiently than the copper cation.

Porphyrin complexes with Mn(III) are more stable than those with Co(II) and Cu(II) and their dissociation rates are two orders of magnitude lower under comparable conditions (see Table 18). However, the character of changes in the dissociation rates depending on the degree of deformation of the porphyrin ligands is the same: on going from octaethylporphine to the tetraphenyl derivative, the dissociation rate constants of the manganese complex increase by three orders of magnitude in a mixture of acetic and trifluoroacetic acids and 60-fold in a mixture of acetic and sulfuric acids. In these media, the manganese complex of dodecaphenylporphine dissociates at immeasurably fast rates.

Studies of axial coordination of piperidine and 1-methylimidazole by zinc complexes of spatially distorted porphyrins (Table 19) have demonstrated that stabilities of these complexes decrease regularly with an increase in the number of peripheral substituents.[95] This supports again an assumption that the deformation of cores in polysubstituted porphyrins decreases the aromaticity of the macrocycle and increases the negative charge

Table 19. Stability constants of axial complexes of zinc porphyrinates with piperidine and 1-methylimidazole in benzene at 298 K.[95]

Metallo-porphyrin	$K \times 10^{-2}$ /litre mol^{-1}	
	for the complex with piperidine	for the complex with 1-methylimidazole
ZnP (**1**)	198 ± 3	223 ± 5
ZnP (**2**)	125 ± 2	147 ± 6
ZnP (**18**)	81 ± 2	79 ± 1
ZnP (**19**)	47 ± 9	53 ± 2
ZnP (**20**)	48 ± 5	48 ± 7
ZnP (**21**)	37 ± 9	38 ± 9
ZnP (**3**)	24 ± 5	25 ± 2

on the nitrogen atom which causes a decrease in the effective positive charge on the coordinating metal cation in the metalloporphyrins.

This review has been written with the financial support of the Russian Foundation for Basic Research (Project No. 03-03-96458-p2003).

References

1. M J Hamor, T A Hamor, J L Hoard *J. Am. Chem. Soc.* **86** 1938 (1964)
2. S J Silvers, A Tulinsky *J. Am. Chem. Soc.* **89** 3331 (1967)
3. E B Fleisher *J. Am. Chem. Soc.* **85** 1353 (1963)
4. J L Hoard *Ann. N. Y. Acad. Sci.* **206** 18 (1973)
5. J L Hoard, in *Porphyrins and Metalloporphyrins* (Ed. K M Smith) (Amsterdam: Elsevier, 1975) p. 317
6. P Hambright. *Coord. Chem. Rev.* **6** 247 (1971)
7. O A Golubchikov, T N Lomova, E M Kuvshinova, S G Korovina, M E Klyueva, Z I Zhilina, B D Berezin *Zh. Fiz. Khim.* **63** 346 (1989) [a]
8. http//www-chem.ucdavis.edu/groups/smith.html
9. A S Semeikin, P A Shatunov, in *Uspekhi Khimii Porfirinov* (Progress in the Chemistry of Porphyrins) (Ed. O A Golubchikov) (St Petersburg: Research Institute of Chemistry, St Petersburg State University, 2001) Vol. 3, p. 47
10. E F Meyer Jr *Acta Crystallogr., Sect. B* **28** 2162 (1972)
11. D L Cullen, E F Meyer Jr *J. Am. Chem. Soc.* **96** 2095 (1974)
12. J W Lauher, J A Ibers *J. Am. Chem. Soc.* **95** 5148 (1973)
13. A L MacLean, G J Foran, B J Kennedy, P Turner, T W Hambley *Aust. J. Chem.* **49** 1273 (1996)
14. T D Brennan, W R Scheidt, J A Shelnutt *J. Am. Chem. Soc.* **110** 3919 (1988)
15. K M Barkigia, J Fajer, M D Berber, K M Smith *Acta Crystallogr., Sect. C* **51** 511 (1995)
16. L D Sparks, C J Medforth, M S Park, J R Chamberlain, M R Ondrias, M O Senge, K M Smith, J A Shelnutt *J. Am. Chem. Soc.* **115** 581 (1993)
17. K M Barkigia, M W Renner, R L Furenlid, C J Medforth, K M Smith, J Fajer *J. Am. Chem. Soc.* **115** 3627 (1993)
18. M W Renner, K M Barkigia, Y Zhang, C J Medforth, K M Smith, J Fajer *J. Am. Chem. Soc.* **116** 8582 (1994)
19. K M Barkigia, M D Berber, J Fajer, C J Medforth, M W Renner, K M Smith *J. Am. Chem. Soc.* **112** 8851 (1990)
20. M Gruden, S Grubišic, A G Coustolelos, S R Niketić *J. Mol. Struct.* **595** 209 (2001)
21. A Hazell *Acta Crystallogr., Sect. C* **40** 751 (1984)
22. R G Ball, K M Lee, A G Marshall, J Trotter *Inorg. Chem.* **19** 1463 (1980)
23. K Henrick, R W Matthews, P A Tasker *Inorg. Chem.* **16** 3293 (1977)
24. C J Medforth, M D Berber, K M Smith, J A Shelnutt *Tetrahedron Lett.* **31** 3719 (1990)
25. J A Shelnutt, X-Z Song, W Jentsen, J G Ma, C J Medforth *Chem. Soc. Rev.* **27** 31 (1998)
26. C J Medforth, C M Muzzi, K M Smith, R J Abraham, J D Hobbs, J A Shelnutt *J. Chem. Soc., Chem. Commun.* 1843 (1994)

27. C J Medforth, J D Hobbs, M R Rodriguez, R J Abraham, K M Smith, J A Shelnutt *Inorg. Chem.* **34** 1333 (1995)
28. C J Medforth, C M Muzzi, K M Shea, K M Smith, R J Abraham, S Jia, J A Shelnutt *J. Chem. Soc., Perkin Trans. 2* 833 (1997)
29. C J Medforth, C M Muzzi, K M Shea, K M Smith, R J Abraham, S Jia, J A Shelnutt *J. Chem. Soc., Perkin Trans. 2* 839 (1997)
30. J L Retsek, C J Medforth, D J Nurco, S Gentemann, V S Chirvony, K M Smith, D Holten *J. Phys. Chem. B* **105** 6396 (2001)
31. P A Shatunov, Candidate Thesis in Chemical Sciences, Ivanovo State University of Chemistry and Technology, Ivanovo, 2002
32. E Porhiel, L Toupet, J Leroy, A Bondon *Tetrahedron Lett.* **43** 8293 (2002)
33. L M Henling, W P Schaefer, J A Hodge, M E Hughes, H B Gray, P E Ellis *Acta Crystallogr., Sect. C* **49** 1743 (1993)
34. D Mandon, P Ochsenbein, J Fischer, R Weiss, K Jayaraj, R N Austin, A Gold, P S White, O Brigaud, P Battioni, D Monsuy *Inorg. Chem.* **31** 2044 (1992)
35. M Nakamura, A Ikezaki *Chem. Lett.* 733 (1995)
36. T G Traylor, S Tsuchiya *Inorg. Chem.* **26** 1338 (1987)
37. S Tsuchiya, M Seno *Chem. Lett.* 263 (1989)
38. P Hoffman, G Labat, A Robert, B Meunier *Tetrahedron Lett.* **31** 1991 (1990)
39. T Wijesekera, A Matsumoto, D Dolphin, D Lexa *Angew. Chem.* **102** 1073 (1990)
40. J F Bartoli, O Brigaud, P Battioni, D Mansuy *J. Chem. Soc., Chem. Commun.* 440 (1991)
41. A M A Gonsalves, R A W Johnstone, M M Pereira, J Shaw, A J F N Sobral *Tetrahedron Lett.* **32** 1355 (1991)
42. P Battioni, O Brigaud, H Desvaux, D Mansuy, T G Traylor *Tetrahedron Lett.* **32** 2893 (1991)
43. Russ. P. 2 139 272; *Byull. Izobr.* (28) (1999)
44. C J Medforth, M O Senge, K M Smith, L D Sparks, J A Shelnutt *J. Am. Chem. Soc.* **114** 9859 (1992)
45. D J Nurco, C J Medforth, T P Forsyth, M M Olmstead, K M Smith *J. Am. Chem. Soc.* **118** 10918 (1996)
46. K M Barkigia, D J Nurco, M W Renner, D Melamed, K M Smith, J Fajer *J. Phys. Chem. B* **102** 322 (1998)
47. M O Senge, W W Kalisch *Inorg. Chem.* **36** 6103 (1997)
48. C J Medforth, M O Senge, T P Forsyth, J D Hobbs, J A Shelnutt, K M Smith. *Inorg. Chem.* **33** 3865 (1994)
49. M O Senge, C J Medforth, T P Forsyth, D A Lee, M M Olmstead, W Jentzen, R K Randey, J A Shelnutt, K M Smith *Inorg. Chem.* **36** 1149 (1997)
50. J P Collman, A O Chong, G B Jameson, R T Oakley, E Rose, E R Schmittou, J A Ibers *J. Am. Chem. Soc.* **103** 516 (1981)
51. K-L Lay, J W Buchler, J E Kenny, W R Scheidt *Inorg. Chim. Acta* **123** 91 (1986)
52. T Nagata, A Osuka, K Maruyama, K Toriumi *Acta Crystallogr. Sect. C* **46** 1745 (1990)
53. T Ema, M O Senge, N J Nelson *Angew. Chem., Int. Ed. Engl.* **33** 1879 (1994)
54. M O Senge, T Ema, K M Smith *J. Chem. Soc., Chem. Commun.* 733 (1995)
55. E K Kairyak, Candidate Thesis in Chemical Sciences, Ivanovo State University of Chemistry and Technology, Ivanovo, 2001
56. D L Kuz'min, Candidate Thesis in Chemical Sciences, Ivanovo State University of Chemistry and Technology, Ivanovo, 2002
57. C J Medforth, K M Smith *Tetrahedron Lett.* **31** 5583 (1990)
58. R J Abraham, G E Hawkes, K M Smith *Tetrahedron Lett.* 1483 (1974)
59. L D Sparks, K K Anderson, C J Medforth, K M Smith, J A Shelnutt *Inorg. Chem.* **33** 2297 (1994)
60. J A Shelnutt, C J Medforth, M D Berber, K M Barkigia, K M Smith *J. Am. Chem. Soc.* **113** 4077 (1991)
61. M Abe, T Kitagawa, Y J Kyogoku *J. Chem. Phys.* **69** 4526 (1978)
62. A B J Parusel, T Wondimagegn, A Ghosh *J. Am. Chem. Soc.* **122** 6371 (2000)
63. T Wondimagegn, A Ghosh *J. Phys. Chem. A* **104** 4606 (2000)
64. S Grimme *Chem. Phys. Lett.* **259** 128 (1996)
65. A B J Parusel, A Ghosh *J. Phys. Chem. A* **104** 2504 (2000)
66. S G DiMagno, R A Williams, M J Therien *J. Org. Chem.* **59** 6943 (1994)
67. J G Goll, K T Moore, A Ghosh, M J Therien *J. Am. Chem. Soc.* **118** 8344 (1996)
68. L A Poveda, V R Ferro, J M de la Vega, R H Gonzalez-Jonte *J. Comput.-Aided Mol. Design* **15** 183 (2001)
69. J A Hodge, M G Hill, H B Gray *Inorg. Chem.* **34** 809 (1995)
70. M W Renner, K M Barkigia, J Fajer *Inorg. Chim. Acta* **263** 181 (1997)
71. A Giraudeau, H J Callot, M Gross *Inorg. Chem.* **18** 201 (1979)
72. T Takeuchi, H B Gray, W A Goddard III *J. Am. Shem. Soc.* **116** 9730 (1994)
73. P Ochsenbein, K Ayougou, D Mandon, J Fischer, R Weiss, R N Austin, K Jayaraj, A Gold, J Terner, J Fajer *Angew. Chem., Int. Ed. Engl.* **33** 348 (1994)
74. F D'Souza, M E Zandler, P Tagliatesta, Z Ou, J Shao, E Van Caemelbecke, K M Kadish *Inorg. Chem.* **37** 4567 (1998)
75. Y Terazono, B O Patrick, D H Dolphin *Inorg. Chem.* **41** 6703 (2002)
76. S Funahashi, Y Inada, M Inamo *Anal. Sci.* **17** 917 (2001)
77. O A Golubchikov, S G Korovina, E M Kuvshinova, A S Semeikin, A M Shul'ga, V A Perfil'ev, S A Syrbu, B D Berezin *Zh. Org. Khim.* **24** 2378 (1988) [b]
78. E M Kuvshinova, O A Golubchikov, B D Berezin *Zh. Obshch. Khim.* **61** 1799 (1991) [c]
79. E M Kuvshinova, S G Pukhovskaya, L Zh Guseva, A S Semeikin, O A Golubchikov *Zh. Fiz. Khim.* **72** 1040 (1998) [a]
80. O A Golubchikov, E M Kuvshinova, S G Korovina, A S Semeikin, S A Syrbu, B D Berezin *Zh. Fiz. Khim.* **63** 912 (1989) [a]
81. E M Kuvshinova, S G Pukhovskaya, O A Golubchikov, B D Berezin *Koord. Khim.* **19** 630 (1993) [d]
82. O A Golubchikov, S G Pukhovskaya, E M Kuvshinova *Zh. Obshch. Khim.* **70** 1719 (2000) [c]
83. O A Golubchikov, S G Pukhovskaya, E M Kuvshinova, in *Uspekhi Khimii Porfirinov* (Progress in the Chemistry of Porphyrins) (St Petersburg: Research Institute of Chemistry, St Petersburg State University, 1999) Vol. 2, p. 27
84. O A Golubchikov, S G Pukhovskaya, Yu P Pukhovskii *Izv. Vyssh. Ucheb. Zaved., Khim. Khim. Tekhnol.* **41** 113 (1998)
85. S G Pukhovskaya, L Zh Guseva, O V Malkova, A S Semeikin, O A Golubchikov *Zh. Obshch. Khim.* **73** 505 (2003) [c]
86. D K Lavallee *Chemistry and Biochemistry of N-Substituted Porphyrins* (Weinheim: VCH, 1987)
87. S A Shushin, V G Andrianov, B D Berezin *Izv. Vyssh. Ucheb. Zaved., Khim. Khim. Tekhnol.* **31** 53 (1988)
88. V G Andrianov, O V Malkova, B D Berezin, in *Uspekhi Khimii Porfirinov* (Progress in the Chemistry of Porphyrins) (Ed. O A Golubchikov) (St Petersburg: Research Institute of Chemistry, St Petersburg State University, 2001) Vol. 3, p. 107
89. O S Finikova, A V Cheprakov, P J Carroll, S Dolosto, S A Vinogradov *Inorg. Chem.* **41** 6944 (2002)
90. B D Berezin *Koordinatsionnye Soedineniya Porfirinov i Ftalotsianina* (Coordination Compounds of Porphyrins and Phthalocyanine) (Moscow: Nauka, 1978)
91. B D Berezin, O A Golubchikov *Koordinatsionnaya Khimiya Sol'vatokompleksov Solei Perekhodnykh Metallov* (Coordination Chemistry of Solvated Complexes of Transition Metal Salts) (Moscow: Nauka, 1992)
92. E M Kuvshinova, N S Dudkina, S G Pukhovskaya, A S Semeikin, O A Golubchikov *Zh. Obshch. Khim.* **70** 1010 (2000) [c]
93. E M Kuvshinova, D L Kuz'min, S G Pukhovskaya, N S Dudkina, A S Semeikin, O A Golubchikov. *Zh. Obshch. Khim.* **72** 142 (2002) [c]
94. O A Golubchikov, N Zh Mamardashvili, A S Semeikin, S A Zdanovich *Koord. Khim.* **20** 747 (1994) [d]
95. S G Pukhovskaya, L Zh Guseva, A S Semeikin, O A Golubchikov, in *IX Mezhdunaradnaya Konferentsiya po Khimii Porfirinov i ikh Analogov (Tez. Dokl.), Suzdal', 2003* [The IXth International Conference on the Chemistry of Porphyrins and Their Analogues (Abstracts of Reports), Suzdal', 2003] p. 25

[a] — *Russ. J. Phys. Chem. (Engl. Transl.)*
[b] — *Russ. J. Org. Chem. (Engl. Transl.)*
[c] — *Russ. J. Gen. Chem. (Engl. Transl.)*
[d] — *Russ. J. Coord. Chem. (Engl. Transl.)*